ISSN: 0001-5113
AADRAY

ACTA ADRIAT.
37 (1/2): 35-68, 1996

UDC: 551.465 (262.3)
Original scientific paper

Ecological study of gas fields in the northern Adriatic

4. Circulation

Mira ZORE-ARMANDA[+], Mario BONE[+], Vlado DADIĆ[+], Miroslav GAČIĆ[+*], Vedrana KOVAČEVIĆ[+*] and Zoran VUČAK[++]

[+]Institute of Oceanography and fishers, Split, Croatia

[++]State Hydrographic Institute, Split, Croatia

[*]Osservatorio Geofisico Sperimentale, Trieste, Italia

In the period from 1978. to 1986. sea currents have been measured from the research platforms in the gas fields IVANA and IKA. Multi-year data sets have been statistically processed and analyzed in relation to the various components of circulation.

4.1. INTRODUCTION

Although the north Adriatic has been very intensively explored from various aspects for several decades, the direct measurements of currents are rather recent. We believe that the comprehensive current measurements data presented in this article will serve as a useful source for the explanation of various aspects of the hydrography of the region. The results of the statistical analysis have been presented, and the currents have been separated to their principal components in relation to the causes:
- Thermohaline circulation which is the consequence of the gradients of temperature and salinity, i.e. the water density: This circulation vary seasonally and it basically appears as residual circulation.
- The circulation caused by the dynamic atmospheric influence. Those are long period waves on the synoptic scale (cca 7 days), and other forms of the drift currents. Inertial oscillations and seiches are also indirectly caused by wind.
- Gravity inertial waves as a consequence of tides in the Adriatic.
- Gravity waves which are basically internal waves connected to the oscillations of the thermocline height.

4.2. MATERIAL AND METHODS

The currents were measured from the research platforms in the period from 1978 to 1986. From 1978 to 1984 the Russian mechanical self-recording current meters ALEKSEJEV, type BPV-2r were used. These recorded direction and the speed at 15 minutes intervals. From September 1984 to 1986 the autonomous AANDERAA instruments were used which recorded direction and the speed within the intervals of 10 minutes. Before introducing the new current meters in 1982, both ALEKSEJEV and AANDERAA were hung in parallel for intercalibration. Later analysis (VUČAK and SMIRČIĆ, 1983) showed the data were well correlated.

In the course of the measurements the gauges were placed at the three layers: surface (mean depth 5 m), intermediary (mean depth for IVANA 20 m, for IKA 30 m) and bottom (mean depth for IVANA 40 m, for IKA 50 m). The research platform changed its position as

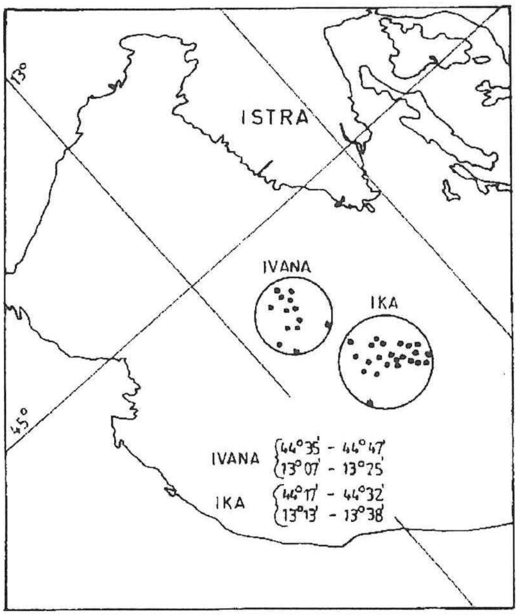

Fig. 4.1. The positions of the research platforms in the fields IVANA and IKA, where current measurements were performed from 1978 to 1986.

shown (Fig.4.1.). The two fields shall be considered as separate data sources. However, each bit of data collected within each field shall be considered as representative of conditions in that entire field. The area of the field IVANA is confined by the circle inside the following coordinates: φ = 44°35' - 44°47'; λ = 13°07' - 13°25', the field IKA by the coordinates: φ = 44°17'- 44°32', λ = 13°13' - 13°38'. The periods of measurements in particular years differ as shown (Figs 4.2. and

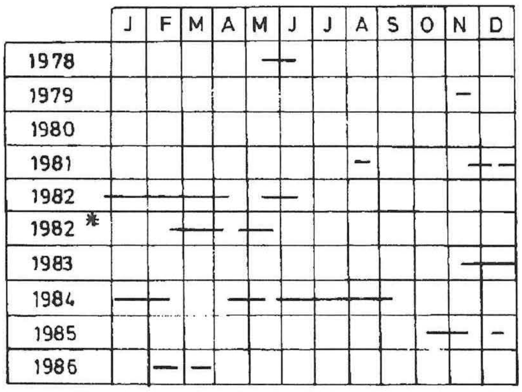

*Fig. 4.2. The periods of measurements in IVANA. Parallel measurements with Aleksejev and Aandera meters marked by * have been performed in 1982.*

4.3.), the result of which are also the different number of data, so the years cannot be well

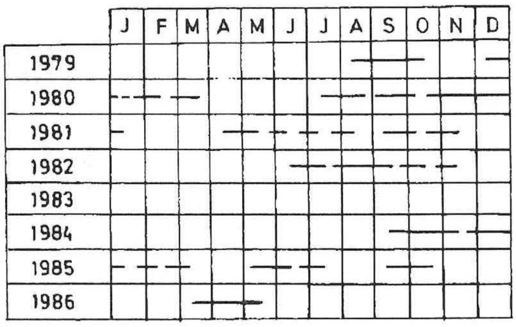

Fig. 4.3. The periods of measurements in IKA.

compared. The total number of data for all the layers in the field IVANA is 168 065 and in the field IKA 284 570. The following values have been calculated from the records (tables 4.A.1.-4.A.6.) :

-mean annual,seasonal and monthly vector speeds;

- mean annual, seasonal and monthly scalar speeds, their standard deviations, minimum and maximum values;
- mean annual, seasonal and monthly values of the north (N) and east (E) component, their standard deviations, minimum and maximum values;
- kinetic energy of the mean currents (annual, seasonal and monthly), of the fluctuations of the currents and their sum. From the time series the average value of kinetic energy $\langle \vec{u}^2/2 \rangle$ and its variance

$$\langle (\vec{u}/2)^2 \rangle^2 - \langle u^2/2 \rangle^2$$

has been determined.

Standard deviation of kinetic energy

$$\sqrt{\langle (\vec{u}/2)^2 \rangle^2 - \langle u^2/2 \rangle^2}$$

presents kinetic energy of fluctuations. The sum of the average value and fluctuations energy gives the total kinetic energy.

- mean annual and seasonal frequency for eight directions, their mean speeds and frequency for the class intervals of 5 cm /s^{-1};

- rotational spectra (spectrum analysis after GONELLA, 1972), for some particular periods.

For data processing the seasons were defined as follows:
Winter: January, February, March,
Spring: April, May, June,
Summer: July, August, September,
Autumn: October, November, December.

Analyzing the measuring data, we noticed that five series of data showed a considerable deviation. This refers to IKA surface currents, measured in November 1980 through January 1981. The series are characterized by the usual current oscillations, but this occurred around extremely high mean value (about 70 cm s^{-1}). Such anomalous speeds, compared to the currents measured before and after that period, and the currents measured in the corresponding seasons of other years suggested that defective instrument was used in the five series of measurements. Upon consideration we concluded instrument has probably been wrongly calibrated. At that point it was not possible to define the quantity of the systematic error, and the quantity necessary to reduce the series, in order to obtain the realistic data. Any effort to estimate reduction in the current speed would be as incorrect as original data so we left the data as registered. The directions, however, appear to be correct.

Since no corrections of those very high speeds could been done, it had to be decided whether to leave those series out of the analysis or include them in, with the remark that the speed values are higher than expected. We analyzed all the data for the surface layer on the location of IKA, both including the five series and excluding them. Comparing the statistical results, we, nevertheless, decided to include the five series, since they do not influence the absolute extreme current values. The differences are evident in the total mean current, seasonal mean current for autumn and winter as well as monthly mean current for November, December and January. Leaving out these five series of data for the surface would at the same time require leaving out the correctly measured series at the intermediary and bottom layer, otherwise the obtained statistical data would be distorted and the surface mean values could not be compared to the corresponding intermediary and bottom values. Excluding the series would result in the blank space for the autumn and winter season. In presenting results the attention will be drawn to these doubtful values.

Lagrange current measurements were made using drift cards, 12.4 cm x 8.8 cm in size, in plastic cover. They were flung from the research platforms - 10 775 pieces - in the period between 1979 to 1986. Out of 3 600 cards from the location IVANA 926 were found. From 7 175 IKA cards 1 335 were found. Each card was identified according to its number, and than filed the time and site it had been found.

4.3. RESIDUAL CIRCULATION

Residual circulation presents a net circulation, that is the current that remains when the periodic components have been subtracted. Mean current for a longer period, i.e. residual current should be well in accordance with the geostrophic circulation. An earlier analysis of the north Adriatic residual circulation (ZORE-ARMANDA and VUČAK, 1984, ZORE-ARMANDA and GAČIĆ, 1987) has been shown. The Fig. 4.4. indicates a cyclonic gyre that occupies much of the northern basin, while to the south there is an anticyclonic gyre, the southern branch of which fits to the general cyclonic circulation of the Adriatic.

Such circulation model was connected to the impact of the river Po and the influence of the typical wind Bora. The IVANA field is placed in the middle of the anticyclonic gyre and the IKA field is in its western current branch. Mean currents vectors for the entire period of measurements in both fields (Fig.4.5.) show western current appears in all three IKA layers, while IVANA is indicated to have northern current in the surface and the intermediary

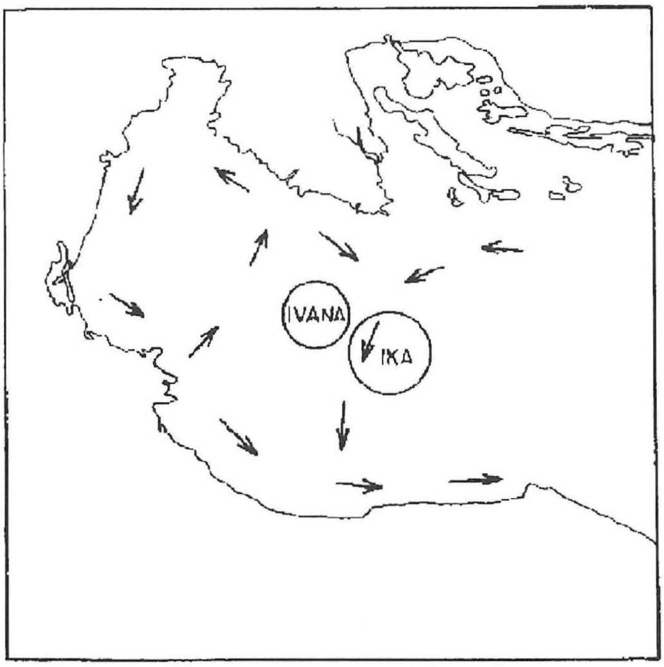

Fig. 4.4. Residual circulation in the north Adriatic (after ZORE-ARMANDA and VUČAK, 1984). The areas of IVANA and IKA are marked.

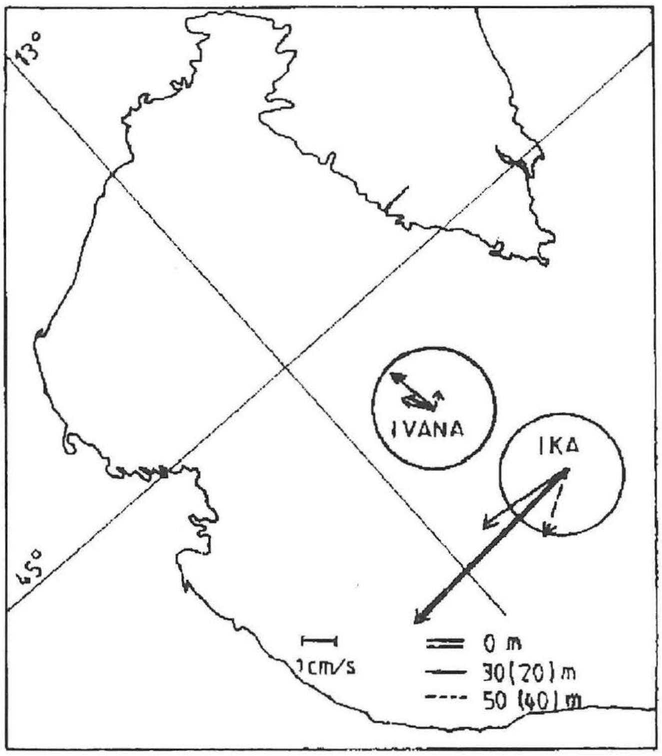

Fig. 4.5. Residual current vectors for IVANA and IKA in three layers: surface (double full line), inter mediary (full line), bottom (hatched line).

layer, and a north-eastern current in the bottom layer. The deviation to the right in lower layers of the field IVANA corresponds to the EKMAN'S spiral.

In the field IKA the residual circulation has a considerably greater speed. Therefrom it is clear that the field IKA lies with its greater part in the permanent western branch of the current. The field IVANA is closer to the center of the gyre, where the direction changes in the course of the year, and this results in a lower residual speed and a variable direction. This is well confirmed by the monthly residual vectors. In the field IKA during all months and at all three layers appears a westerly or a southwesterly current. The only exception are the two winter months in the intermediary layer and one summer month in the bottom layer (Fig. 4.6.). Conversely, the field IVANA shows vectors that are oriented in different directions and speeds according to the months of the year. The seasonal variations in the field IVANA are more clearly shown by the seasonal resultants (Fig.4.7.). In each season the resultant direction appears to be different. In summer and winter the flow is vertically homogeneous, while in the other seasons it changes with depth. In spring the direction changes between the surface and intermediary layer, and in autumn between the intermediary and the bottom layer. On the contrary, in the field IKA the winter current at the intermediary level is different to the surface and bottom level. The current in summer is vertically homogeneous, as in IVANA. Note also some monthly vectors (June, July, August) having oposite directions in each field, which gives possibility of divergence in between two areas.

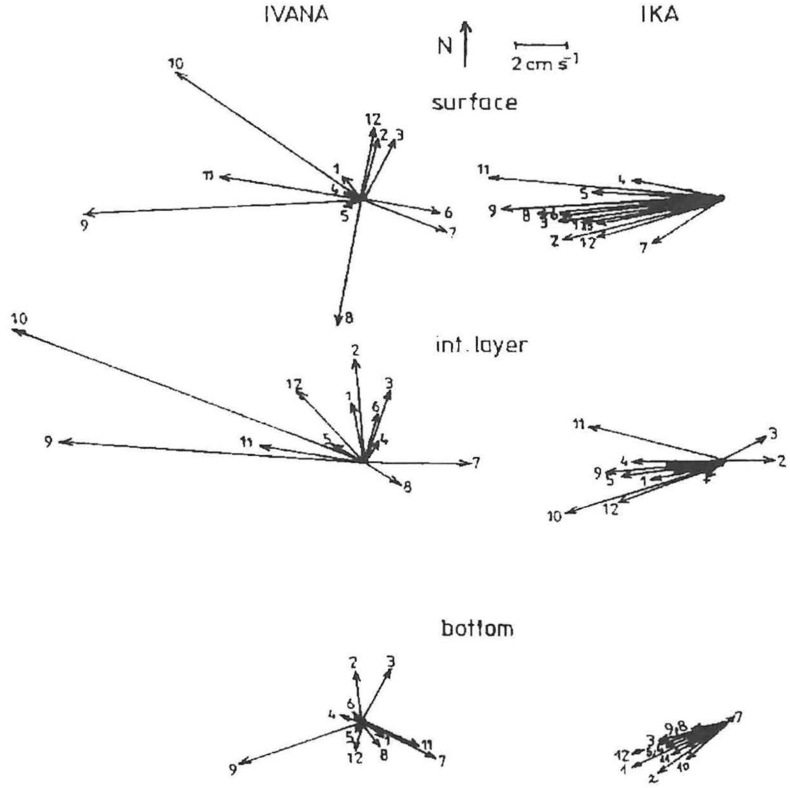

Fig. 4.6. Monthly residual vectors for the entire period in IVANA and IKA for surface, intermediary and bottom layers. Months are indicated by numbers.

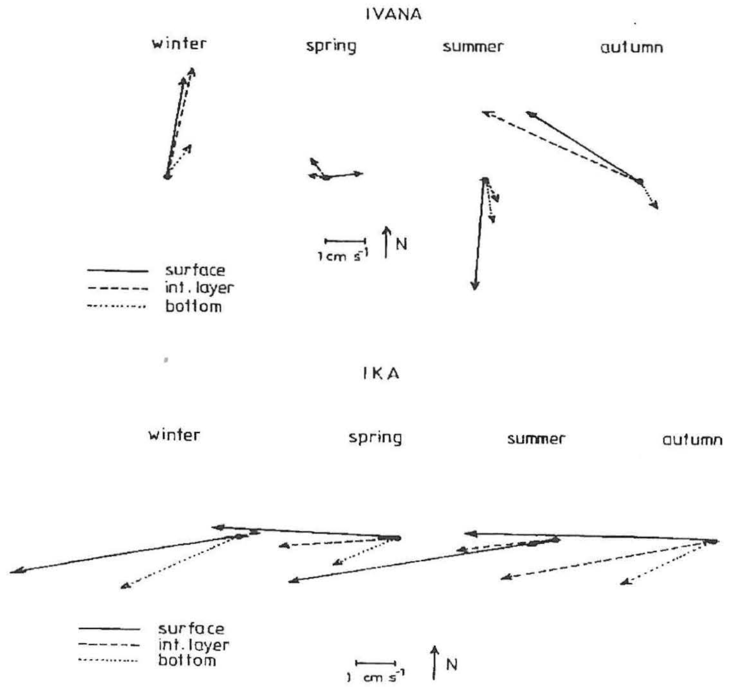

Fig. 4.7. Seasonal residual vectors for the entire period in IVANA and IKA for surface, intermediary and bottom layers.

The mean monthly variations of northern and eastern current components clearly expose differences between IVANA and IKA (Fig. 4.8.). Both components in IKA show considerably lower variation. The most significant changes in the annual course in IVANA occur from August to November in the eastern component. The important differences at various levels occur in IVANA in autumn, in IKA in winter. However, the residual current on both fields is basically vertically homogeneous (one-layer system).

In IVANA the seasonal directions resemble to the seasonal directions of the geostrophic circulation of the open Adriatic (Fig.4.9.). According to ZORE-ARMANDA (1966), the ingoing (north-western) current to the Adriatic prevails in winter. In summer it is the outgoing south-eastern current, while in spring and autumn the transverse current between two coasts prevails. This scheme appears to hold truth in IVANA, whose seasonal residual vectors mostly correspond to the geostrophic circulation. BRANA and KRAJCAR (1995) analyzing the data from the nearby station B (see Fig.1.2.) also found different current direction in summer compared to the rest of the year. In IKA, the geostrophic, as well as the residual circulation, in all the seasons, are all oriented westward (MOSETTI and LAVENIA, 1969, BULJAN and ZORE-ARMANDA, 1976).

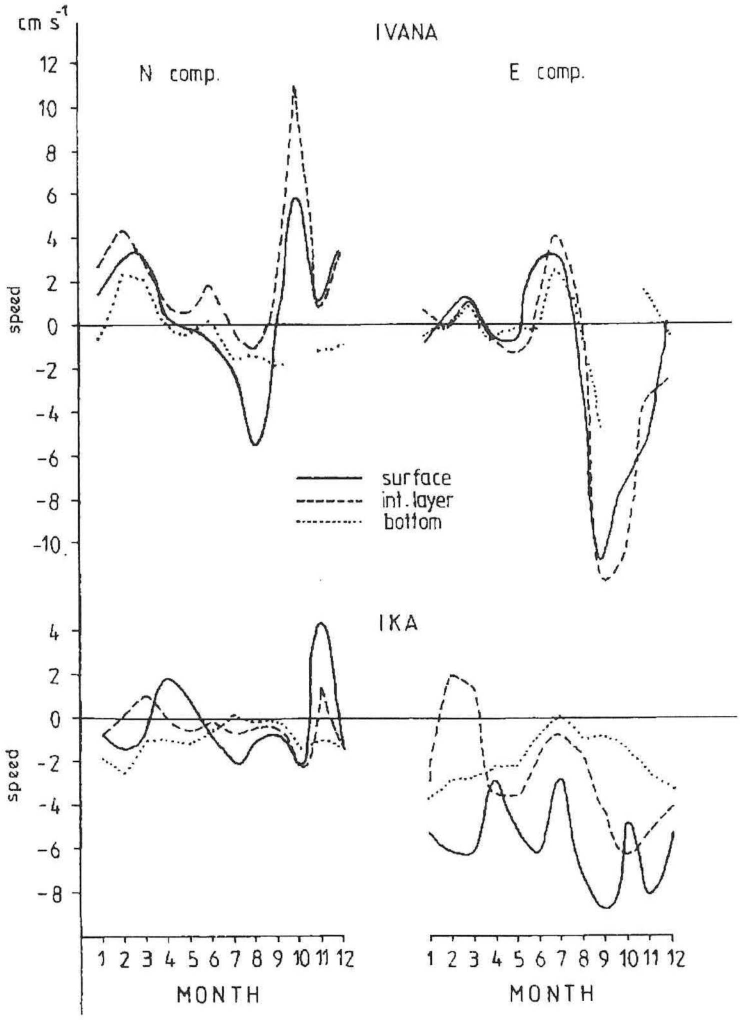

Fig. 4.8. Annual variation of the north and east current component based on the entire period of mea surements in IVANA and IKA for surface, inter mediary and bottom layers.

The relationship between the fluctuations kinetic energy and the mean current kinetic energy could be understood as the measure for the share of mean current in the current field, so the parameters can be related.

The mean currents kinetic energy was low in comparison to the kinetic energy of fluctuations (Table 4.1). This indicates that the currents field was dominated by the oscillations. On average the IKA mean kinetic energy is slightly higher than IVANA, which also indicates that the IKA currents are more stable than IVANA. In IVANA the highest mean currents kinetic energy value, as well as the highest residual speed, appears in September and

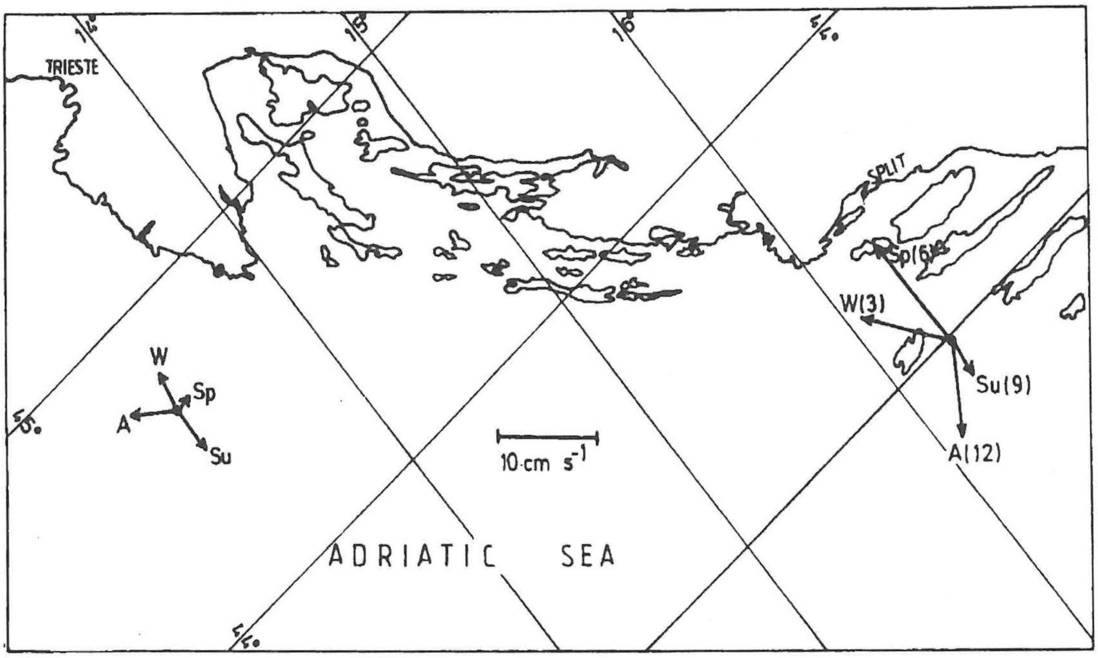

Fig. 4.9. Seasonal currents residual vectors for the suface layer in IVANA and in the permanent station Stončica in the middle Adriatic (after ZORE-ARMANDA, 1966).

October, at all three levels, and it is also high in the period from August to November. The IKA field is also high for the same period, but in the surface level it is high in November, at the intermediary level in October, and at the bottom level again in November. Comparing the table 4.A.3. and 4.A.4. with the Fig. 4.8. shows that in both fields the mean currents energy increases with the increase of the western component of currents in all the layers.

The kinetic energy of fluctuations decreases from the surface to the bottom (Table 4.1.). The highest monthly values of the fluctuations kinetic energy appear at the same time with the highest values of the scalar speeds. In IVANA this occurs from May to September, with peak at the surface level in June, at the intermediary level in August and at the bottom level in September. In IKA the higher values of the surface and bottom levels also appear in June, the highest being from November to January. At the same time, in IVANA, from May to September, and in IKA in July, the eastern current component is more intense (Fig.4.8.).

Table 4.1. The currents kinetic energy (10^{-4} m^2 s^{-2}) for the whole period of measurements and the range of mean monthly values (in brackets).

Layer	Field	Kinetic energy of mean current		Kinetic energy of fluctuations		Total kin. energy	
Surf.	IVANA	1	(0 - 58)	113	(33 - 233)	114	(34 - 238)
	IKA	17	(6 - 42)	260	(65 - 667)	277	(85 - 682)
Interm	IVANA	2	(0 - 116)	73	(35 - 161)	75	(35 - 230)
	IKA	4	(0 - 22)	64	(42 - 93)	68	(43 - 114)
Bott.	IVANA	0	(0 - 13)	27	(18 - 47)	27	(18 - 60)
	IKA	2	(0 -9)	38	(25 -54)	40	(28 -54)

It can be assumed that this fluctuations occur under the influence of inertial oscillations, that exists in the warm part of the year, mostly at the surface, but somewhat weaker in lower layers as well (GAČIĆ and VUČAK, 1982). This is well illustrated in Fig. 4.10., which shows the energy spectra for the stratification interval (warm part of the year) and the interval of vertical homogeneity (cold period). In the period of stratification the predominant oscillation lasts for 17 hours (inertial oscillation), but there are also a number of oscillations of shorter periods, which do not exist in the time of vertical homogeneity.

In IKA the high values of the fluctuations kinetic energy appear in November, December and January, together with the occurrence of outstanding maximum values of all the components of the current. It can be assumed that those are the long period oscillations, connected to the synoptic perturbations (GAČIĆ, 1983). This is confirmed by the energy spectrum for the autumn period (Fig. 4.11.).

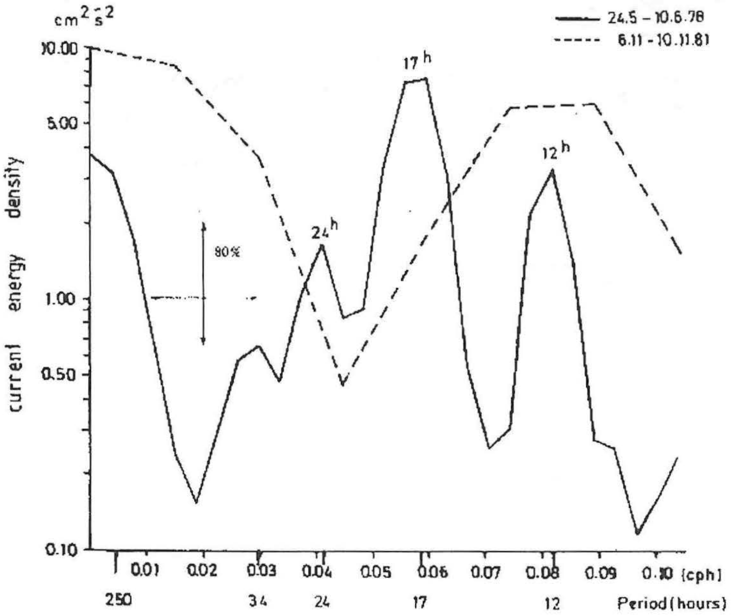

Fig. 4.10. Current energy spectra for the field of IVANA during the period of stratification (24.5. - 10.6.) and the period of vertical homogeneity (6. - 10.11.).

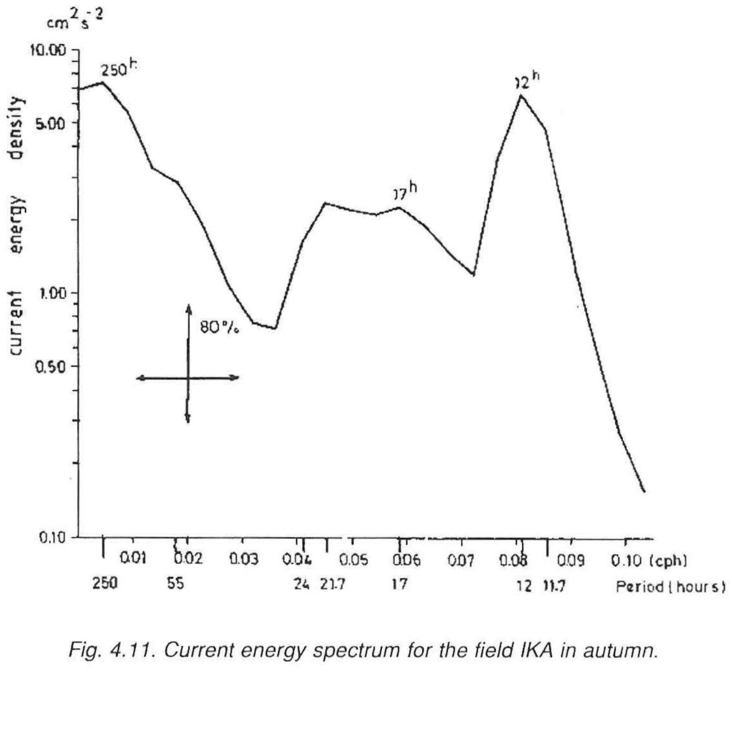

Fig. 4.11. Current energy spectrum for the field IKA in autumn.

4.4. THE FREQUENCY OF DIRECTIONS AND SPEEDS

Corresponding to the residual vectors, the most frequent direction in the surface layer in IKA is the west. In IVANA the most frequent residual direction is to the north and north-west (Fig. 4.12.). The same directions remain equally frequent in the bottom layer. Moreover, in both fields very frequent are also the longitudinal directions NW - SE. They dominate at the lower levels. If we assume that those are the directions of barotrophic tidal currents, their influence increases in the deeper depths where the influence of other types of currents decreases. The longitudinal polarization of directions (NW - SE) in the bottom layer can also be considered as the increased influence of the sea bed to the currents.

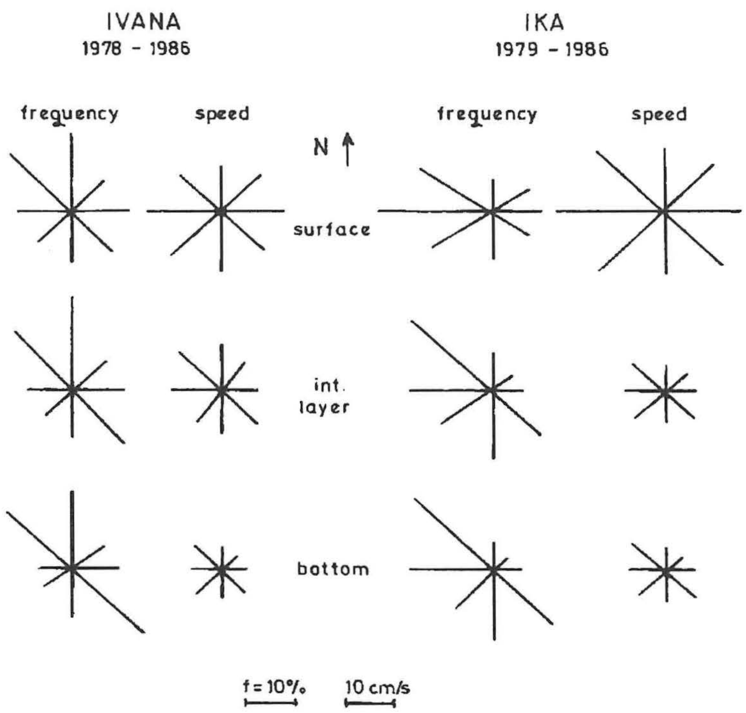

Fig. 4.12. Eight direction current frequencies, in percentages, and their mean speeds for the entire period of measurements in IVANA and IKA for the surface, intermediary and bottom layers.

Table 4.2. The frequency of north and south currents directions in IVANA, given in percentages (%).

	Surface layer		Intermediary layer		Bottom layer	
	N	S	N	S	N	S
Winter	23	8	29	6	23	6
Spring	13	14	16	10	17	15
Summer	5	14	13	11	16	15
Autumn	19	7	17	12	8	14

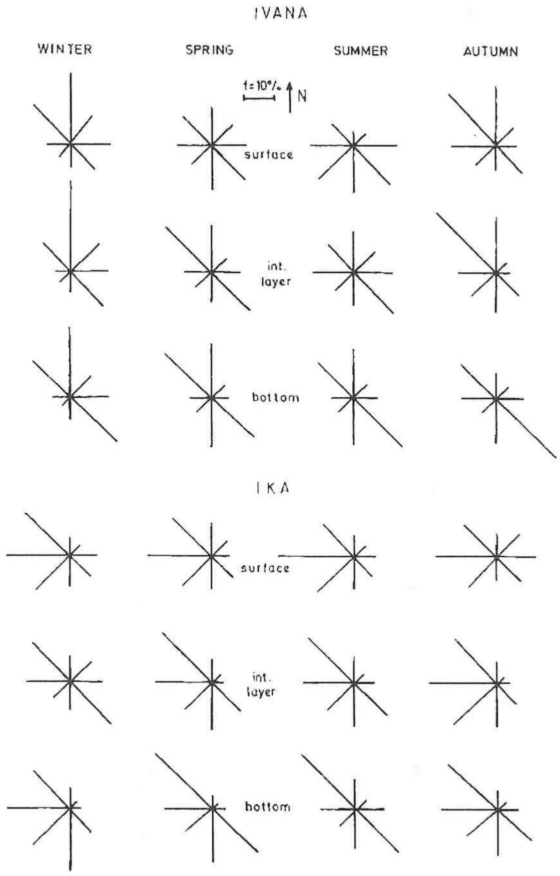

Fig. 4.13. Eight direction current frequencies for four sea sons according to the data from the entire period of measurements in the fields IVANA and IKA).

The outstanding seasonal variations in IVANA are also evident for the directions N - S (Table 4.2., Fig. 4.13.). In winter north is predominant, in spring north and south become equal. In summer the dominant direction is S, which decreases in autumn, while N increases. In deeper layers such relationship is not distinctive. In the IKA field the W direction is dominant in all the seasons.

The surface mean and maximum speeds in the IKA field are higher than in IVANA. At the lower levels they are nearly equal.

Table 4.3. The range of mean scalar and maximum scalar currents speed in cm s^{-1} in the fields IVANA and IKA. The months are given in brackets.

Field	Layer	Mean monthly scalar speed	Annual mean val.	Standard deviation	Maximum monthly scalar speed
IVANA	Surf.	6.9 (1) - 18.5 (7)	12.5	8.4	28.0 (1) - 70.0 (6)
	Int.	7.9 (1) - 19.0 (10)	10.1	6.9	28.0 (11) - 58.0 (8)
	Bott.	5.1 (1,4,6) - 9.2 (9)	6.1	4.1	20.0 (4) - 37.0 (8)
IKA	Surf.	11.1 (5) - 18.5 (7)	17.8	15.4	31.0 (2) - 88.0 (12)
	Int.	7.9 (8) - 26.2 (12)	9.8	6.2	23.0 (5) - 56.0 (10)
	Bott.	6.1 (7) - 8.6 (6)	7.5	5.0	20.3 (4) - 46.0 (10)

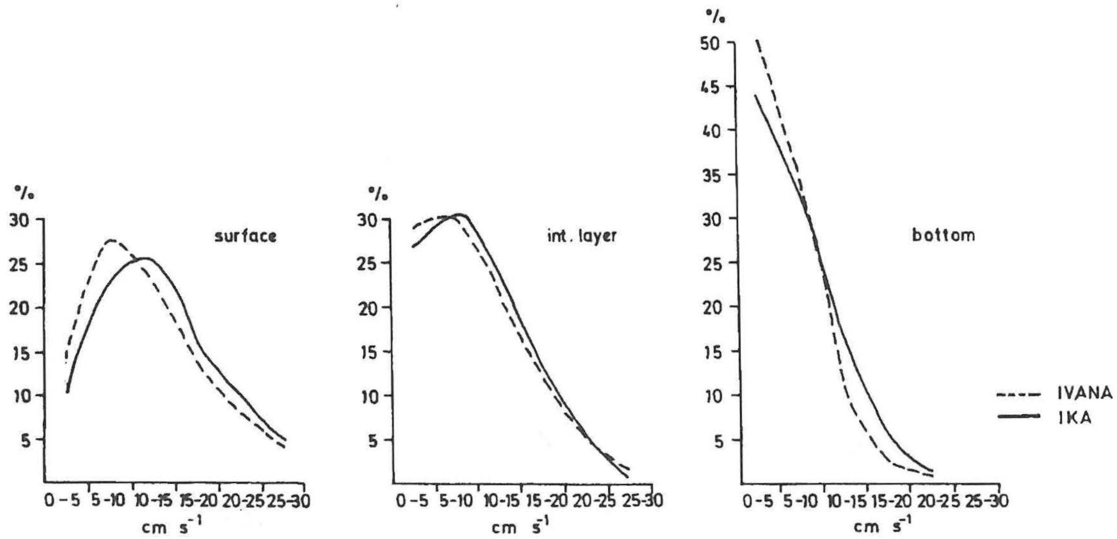

Fig. 4.14. The percentage of the classes of currents speeds (intervals of 5 cm s^{-1}) for the entire period of measurements in the surface, intermediary and bottom layers.

In IVANA the dominant speeds in the surface and intermediary layer are of the class interval 5 - 10 cm s^{-1}, while at the bottom layer they are of the class interval 0 - 5 cm s^{-1}. In the IKA field in the surface layer the dominant speeds are of the class 10 - 15 cm s^{-1}, in the intermediary layer of the class 5 - 10 cm s^{-1}, and in the bottom layer of the class 0-5 cm s^{-1}. The vertical distribution of the speed classes is similar both in IVANA and IKA (Fig. 4.14.). In the IVANA surface layer lower classes are more frequent and higher classes, are less frequent than in IKA. There is a similar relationship in the intermediary and bottom layers, although less distinctive. It can be concluded that higher classes of speeds are more frequent in all the three layers in the field IKA. The seasonal changes of scalar speeds are intensive, especially in the field IVANA.

The mean scalar speeds in IKA have higher values than in IVANA for the three seasons (winter, spring, autumn). However in summer IVANA has higher speeds at all depths. This could be related to the inertial oscillations and their frequency in summer. The highest scalar speed in IKA appears in autumn, but only in the surface and the intermediary layer. This probably happens under the influence of long period oscillations appearing in that season. They also have their influence in January, which can be noticed from the higher winter mean scalar speed in IKA compared to IVANA (Table 4.4.).

Table 4.4. Mean seasonal scalar speeds in the fields IVANA and IKA (given in cm s^{-1}).

Season	Surface layer		Intermediary layer		Bottom layer	
	IVANA	IKA	IVANA	IKA	IVANA	IKA
Winter	9.7	16.3	8.9	9.1	5.6	7.9
Spring	13.9	14.9	8.1	9.0	5.6	7.6
Summer	17.3	16.4	15.0	9.2	8.0	6.7
Autum	12.2	21.8	11.4	11.6	6.5	7.8

In IVANA lower class speeds dominate in winter, then autumn, spring and eventually summer, which means that the lowest speeds appear in winter and the highest in summer (Fig. 4.15.). At the intermediary and bottom layer the sequence is following: spring (lower class speeds prevailing), winter, autumn and summer (higher class speeds prevailing). In IKA both in spring and winter there is a higher percentage of lower class speeds at all the levels, while in summer and autumn higher class speeds prevail.

In the IVANA field the most frequent directions do not show the highest speeds. The highest speeds refer to the directions of W and NW. In IKA the highest speed is most frequent with the direction of W.

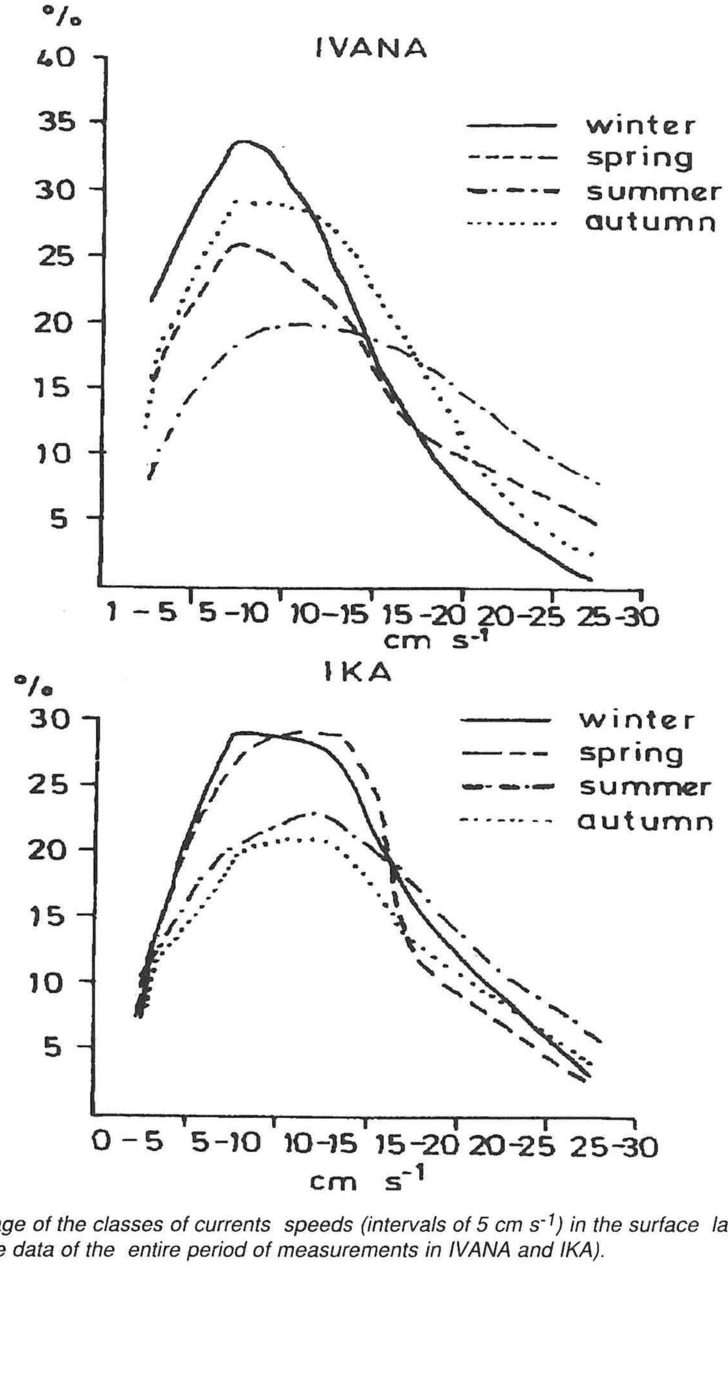

Fig. 4.15. The percentage of the classes of currents speeds (intervals of 5 cm s^{-1}) in the surface layer for the four seasons from the data of the entire period of measurements in IVANA and IKA).

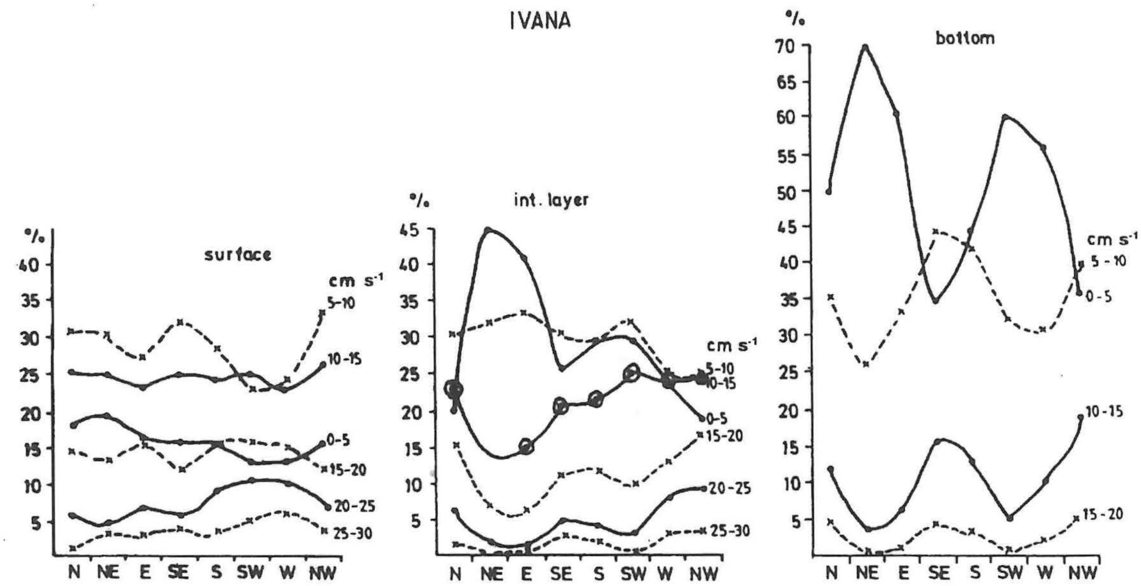

Fig. 4.16. The percentage of the classes of currents speeds (intervals of 5 cm /s^{-1}) for eight directions for the surface, intermediary and bottom layer for the entire period of measurements in IVANA.

Table 4.5. shows the distribution of lower and higher class speeds, according to their directions. Lower class speeds in the surface layer are between 0 - 15 cm s^{-1}, and in the deeper layers they are between 0 - 10 cm s^{-1}.

Table 4.5. The dominant directions of lower class speeds in the fields IKA and IVANA, given for the entire period and for the seasons.

The prevailing directions of lower class speeds

	Surface layer		Intermediary layer		Bottom layer	
	IVANA	IKA	IVANA	IKA	IVANA	IKA
Entire period	SE, N, NW	N, NW, S, (SE)	NE, E, SW	E, NE	NE, SW	NE, SW
Winter	SE, NW	N, S	NE, E	SW, N	NE, SW	NE, E
Spring	SW, W	N, S	NE, SW	E, N	NE	NE, SW
Summer	SE, N, NE	N, NE	NE, SW	E, NE	NE, E	NE, SW
Autumn	SE, N, S	N, SE	NW, E	E, NE	NE, SW	NE, N

The prevailing directions of higher class speeds

	Surface layer		Intermediary layer		Bottom layer	
	IVANA	IKA	IVANA	IKA	IVANA	IKA
Entire period	W, SW	W, E	W, NW, N	NW, W	NW, SE	NW, SE
Winter	W, SW	W, E	W, NW, N	NE	NW, N	NW, W
Spring	E, S	W, NW	W, NW, SE	NW	NW, SE	NW, SE
Summer	W, NW, E	W, SE	W, N, SE	NW, SE	SE	NW, SE
Autumn	W, SW	W, E, NE	W, NW	NW, W, SW	NW, SE, S	NW, SW

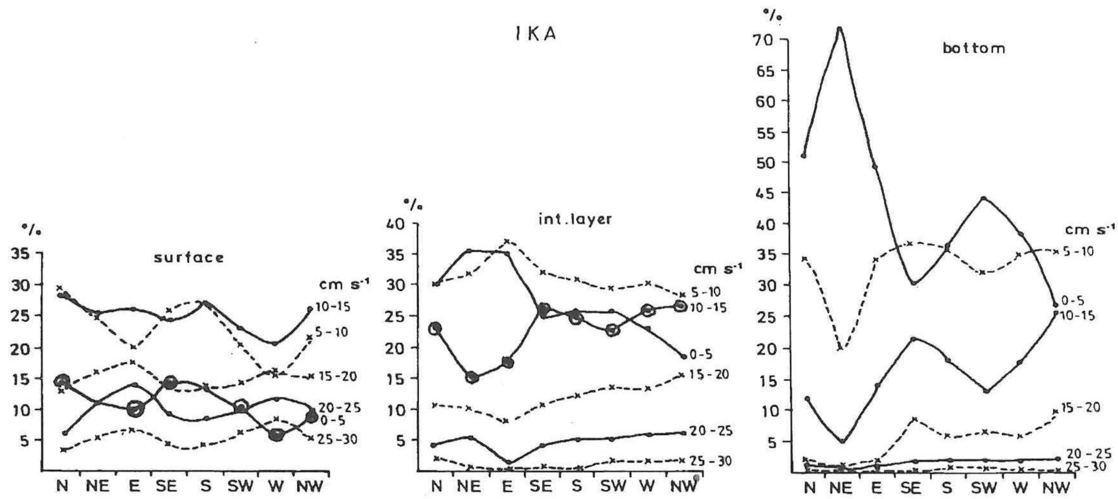

Fig. 4.17. The percentage of the classes of currents speeds (intervals of 5 cm s^{-1}) for eight directions for the surface, intermediary and bottom layers for the entire period of measurements in IKA.

The higher percentage of lower class speeds at the surface level is connected to the directions of SE and NW on both fields. The same directions with higher percentage of high class speeds appear at the bottom level. Figs. 4.16. and 4.17. show various class intervals for speeds according to their directions. Interesting is a regularity related to the SE and NW. The two directions appear with the same percentage in almost all speed intervals. This characteristic is best illustrated in the bottom layer of the field IVANA (Fig. 4.16.): both directions in the class 0 - 5 cm s^{-1} appear at minimum percentage (35%), while in other classes both directions have peak. It has already been mentioned that those are the directions of the tidal currents and here also they show the strong relationship.

The tidal currents in the surface layer have lower speeds in relation to the other types of circulation, while in the intermediary and bottom layer they have the highest speeds. To some extent the N direction acts in a similar way. At the surface and intermediary level on both fields the west direction appears with a higher percentage of higher class speeds.

A higher percentage of lower class speeds in the intermediary layer appear with the directions of NE and SW in both fields. Those two directions show similarities in the distribution of speeds in the same way as the pair of directions of NW and SE. There are also some indications which show that the directions connected to the east component are related to the increase of fluctuations in the current field. The following table shows the connection of certain current directions to the certain class speeds and possibly to particular types of circulation.

It is evident that on both fields in all three layers the lower class speeds most often appear with the directions N, NE, E and SE, while the higher class speeds appear with the directions NW and W.

Table. 4.6. Directions appearing with lower and higher class speeds in three or four seasons.

	Surface layer		Intermediary layer		Bottom layer	
	IVANA	IKA	IVANA	IKA	IVANA	IKA
Lower class speeds	SE	N	NE	E	NE	NE
Higher class speeds	W	W	W, NW	NW	NW	NW

4.5. OSCILLATIONS IN THE CURRENT FIELD

The previous chapter has shown that oscillations produce the major part of the current energy. The periods of oscillations vary from several hours to several days.

A simple way of approximate calculations of the share of periodic currents, is to subtract the daily residual vector from the hourly vectors. In the first approximation by such simple filtering the 24-hour tidal periodic currents have been obtained. However, such a filtration has not eliminated certain periods: inertial oscillations (17 h), and free oscillations of longer periods, so they were partly included in the calculation results. The share of the so obtained periodic oscillations in the entire circulation (the periodicity factor) has also been calculated (Table 4.7.).

The approximative values in the table show the speeds of tidal currents which are in average of several cm s^{-1}, but can also reach high values. Most probably the high speeds correspond to the periods when the inertial oscillations are superimposed onto the tidal currents. The periodicity factor shows a high share of 24-hour periodic currents in the current field. There is an outstanding increase of the periodicity factor with depth, which is in proportion with a relatively increased influence of the tidal currents in deeper layers.

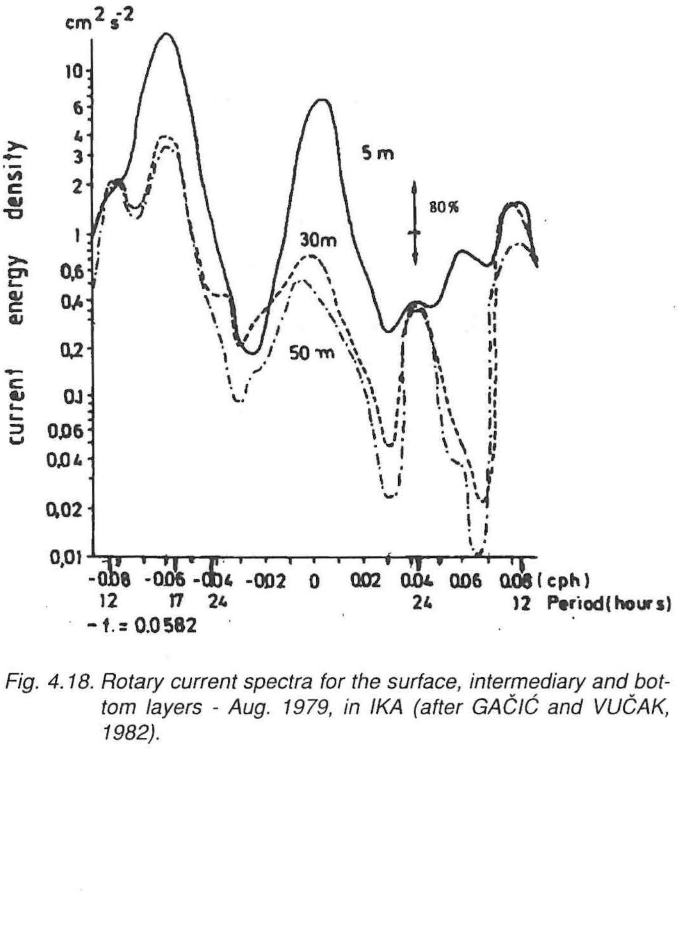

Fig. 4.18. Rotary current spectra for the surface, intermediary and bottom layers - Aug. 1979, in IKA (after GAČIĆ and VUČAK, 1982).

The spectral analysis offers a clear insight to the oscillations of various periods. A typical spectrum is shown in Fig. 4.18. The negative frequency refers to the anticyclonic rotation, while its positive counterpart refers to the cyclonic rotation.

The spectral analysis shows that in summer the peak is at the inertial frequency (17h) and at the negative frequencies only (anti-

Table 4.7. The range of mean monthly and maximum speeds of the 24-hour periodic currents based on all the measurements in both fields for the period 1979-1980

Sea layer	Mean speed cm s^{-1}	Standard deviation cm s^{-1}	Maximum speed cm s^{-1}	Periodicity factor %
Surface	3.3 - 12.2	3.1 - 8.5	15.7 - 52.5	34 - 80
Interm.	3.9 - 11.3	3.6 - 6.6	14.1 - 33.6	41 - 88
Bottom	3.1 - 7.7	2.1 - 5.0	7.5 - 41.9	65 - 96

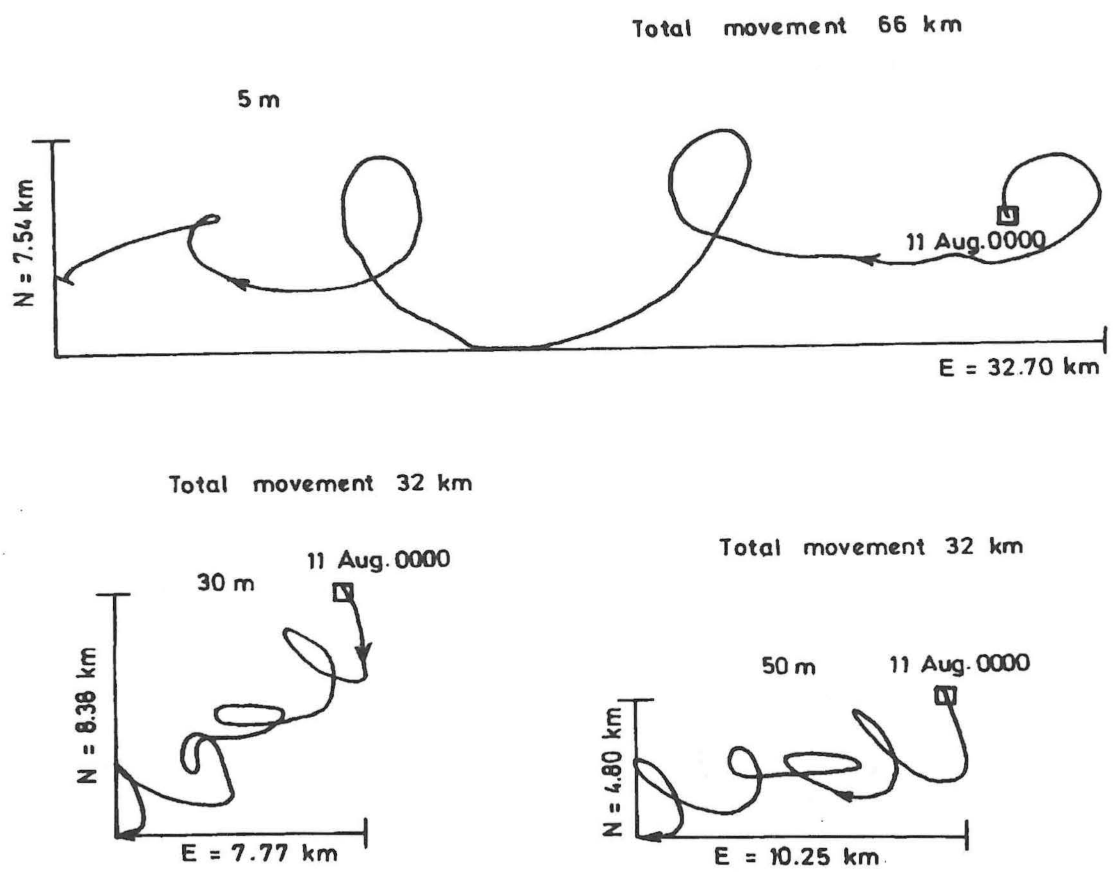

Fig. 4.19. Progressive vector diagram of currents (hourly values), for the period Aug. 11^{th} (0.00h) -Aug. 13^{th} 1979, for the surface, intermediary and bottom layer on IKA.

cyclonic rotation). Earlier investigations showed that in summer the greatest portion of the wind energy induced to the current field of the open sea transforms to the oscillations of the inertial period (GAČIĆ, 1980, 1983). The inertial oscillations appear only in warm seasons, although in winter the wind is stronger. This means that the critical factor for the appearance of such oscillations is the vertical stratification of the sea-water density, which is typical for summer. This is the reason for a considerably higher energy of the oscillations in the surface layer, compared to the ones in the deeper layers. The energy of the oscillations in the intermediary layer (30 m) and the bottom layer (50 m) is roughly equal.

Fig. 4.19. shows the progressive vector diagram for the same interval as in Fig. 4.18., illustrating the rotation of the current vector influenced by the inertial oscillations. At the beginning of the interval a stronger wind appeared, and its force frequently changed within the intervals of several hours. Episodes with strong wind lasted less than 12 hours. Such weather conditions with a high variability of the wind speed easily generate oscillations of the inertial period. The generated anticyclonic 17h oscillations at all the sea levels can be clearly seen in the diagrams. They have been superimposed to the mean flow having W direction in the surface layer, SW in the intermediary layer and WSW in the bottom layer in the course of three days. This proves that oscillations induce current directions different from the W direction.

Fig. 4.20. shows the spectra for the north and east component and for the same time interval in the surface layer. The spectra for

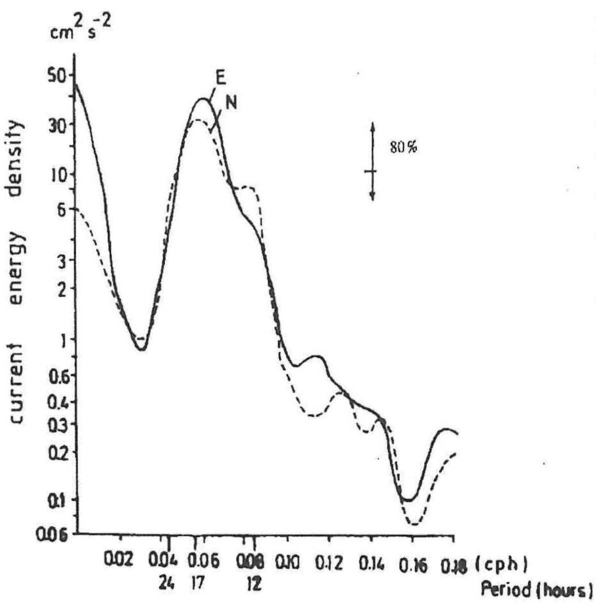

Fig. 4.20. North and East current component spectra for the surface layer in IKA in August 1979.

other layers show the similar characteristics. The oscillation energies at the inertial frequency are of roughly equal values for both components, which also shows that a motion at that frequency is rotational.

Fig. 4.18. shows that around the frequency zero high peak appears, but it has no clear physical meaning, as the data trend was not removed prior to spectral analysis. It probably presents the long period variation in the current field in the time scale longer of several days. Oscillations having period of several days are closely connected to the changes in the wind field on the synoptic scale.

Previous investigations have shown that in summer such oscillations dominate in the region close to the coast (GAČIĆ, 1980, 1983). Further off the coast the share of the long period oscillations in the spectrum of the current field decreases, the same referring to the fields IVANA and IKA. Different situation is in winter when the wind energy spreads to a larger zone from the coast, so inducing much weaker flow. That is the reason why the oscillations with the period of several days caused by the wind are of relatively low energy, similar to the energy of tidal oscillations (Fig. 4.11.). Comparing the spectra of the north and east components (Fig. 4.20.) we can notice that the greater part of energy around zero frequency is within the east component. This means that the long period oscillations in the IKA field appear mostly in the E - W directions, that is parallel to the isobates. At the same typical spectrum (Fig. 4.18.) we can notice the peaks at the tidal frequencies, that is on the periods of 12 and 24 hours. The peak in the 12 hours period has generally a higher energy, but both peaks are remarkably lower from the oscillations at the inertial period. Tidal oscillations are more important at positive frequencies (cyclonic rotation). That is the reason why in winter, when there are no inertial oscillations, the progressive diagrams of periodic currents hourly vectors have, as a rule, a cyclonic rotation.

For a better understanding of the influence of tides in the current field, the currents induced by the tidal force of a known period (12h and 24h) have also been determined by the application of the harmonic analysis. Such circulation, which changes harmonically, can be presented by hodographs, using the method of the rotational components (GONELLA, 1972). The idea of the rotational spectral analysis is to separate the current vector to two vectors of permanent intensity, one rotating in the positive and the other in the negative direction. The result is the ellipse, whose long semi-axis equals to the sum of the rotational vectors intensity, while the short semi-axis equals to the difference of the rotational vectors intensity. The time series of current measurements are long enough to separate from them the five principal harmonic components, induced by the tidal cycle.

These are (e.g. DEFANT, 1961, 267p.):

- M2 - Principal lunar, the period of 12.42 solar hours
- S2 + D2 the sum of principal solar and the luni-solar semi diurnal, the period of 12.00 hours
- N2 - Larger lunar elliptic, the period of 12.66 hours
- Kl + Pl - The sum of luni-solar diurnal and principal solar diurnal, the period of 24.00 hours
- 01 - Principal lunar diurnal, the period of 25.82 hours

Table 4.8 Rotational components of the tidal currents for the three sea layers in the IKA field for the period Aug.10th - Oct.17th 1979, according to BONE, 1988.

Sea layer	Harmonic component	Period	Current amplitude of positive rotation cm s^{-1}	Current amplitude of negative rotation cm s^{-1}	Azimuth of the long el. axis grad.
Surf.	M2	24-hour	2.9	2.4	131
	S2 + K2	12-hour	1.3	1.2	125
	N2	12-hour	0.5	0.3	149
	K1 + P1	24-hour	1.2	0.8	109
	O1	24-hour	0.4	0.1	143
Inter.	M2	12-hour	2.1	2.1	134
	S2 + K2	12-hour	1.2	1.2	133
	N2	12-hour	0.2	0.2	109
	K1 + P1	24-hour	1.1	1.0	125
	O1	24-hour	0.5	0.3	92
Bott.	M2	12-hour	2.2	2.5	134
	S2 + K2	12-hour	1.1	1.2	128
	N2	12-hour	2.1	2.0	142
	K1 + P1	24-hour	0.4	0.8	75
	O1	24-hour	0.7	0.6	153

The tidal currents speeds are low. The approximate speed of the sum of all the components in the surface layer is about 5 cm s^{-1}. The tidal currents speed does not change with the depth. The 12-hour component is more prominent than the 24-hour component, which can also be seen on the spectra (Figs. 4.10., 4.18. and 4.20.).

The currents of single tidal components have been shown in the hodographs (Figs 4.21. - 4.23.). They show that the circulation caused by tides has been polarized in the direction of the coastline (NW - SE), and as a rule it is cyclonic and barotrophic, i.e. independent of the depth. Applying the results of the theoretical analysis of tidal currents profile influenced by the turbulence (TEE, 1979; BONE, 1986) in the open sea the tidal currents profile corresponds to the one caused by the coefficient of the vertical exchange of the momentum of the value 102 cm^2 s^{-1}, i. e. the hodographs from the surface and the bottom layer have the different rotating directions. This has been shown in Fig. 4.21. for the M2 tidal currents component. In the spectrum of the two components (Fig. 4.20.) we can also notice several weaker peaks at the lower periods, which have probably been caused by free oscillations. The peak for the period of about 8.8 hours would correspond to the period of the seiches noticed in the oscillations of the sea level (STRAVISI, 1973). The lower peaks on the periods of 5.8, 5.0, 3.7 and 2.7 hours can also be classed into the same group of oscillations. The free oscillations of the periods of 22 and 11 hours have usually not been distinctive, because of higher peaks of the close tidal oscillations. The oscillation of approximately 22 hours can be noticed in the autumn spectrum (Fig. 4.11.).

To evaluate the relative importance of the observed oscillations in the current field, the kinetic energies for he various periods of oscillations have been calculated (Table 4.9.). The energies for a certain period interval have been separated by the moving averages (using boxcar filter). By applying the 14-day moving average it was possible to separate the residual circulation of the long period waves. By applying the 48-hour moving average, it was possible to separate the residual circulation

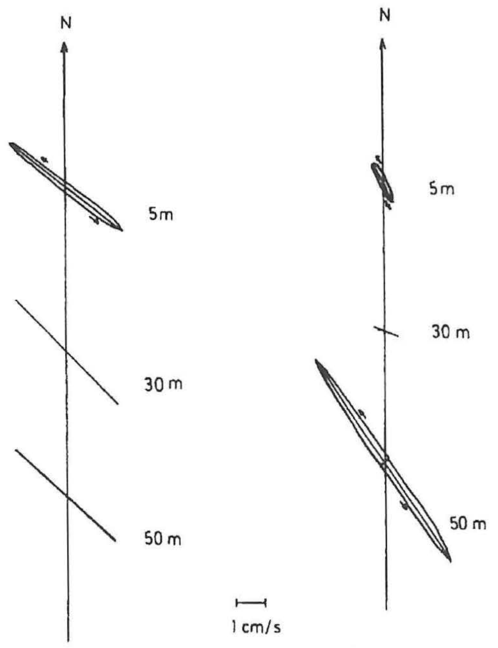

Fig. 4.22. Hodographs of the S2 + K2 tidal current components (left) and N2 component (right) for the surface, intermediary and bottom layer in IKA.

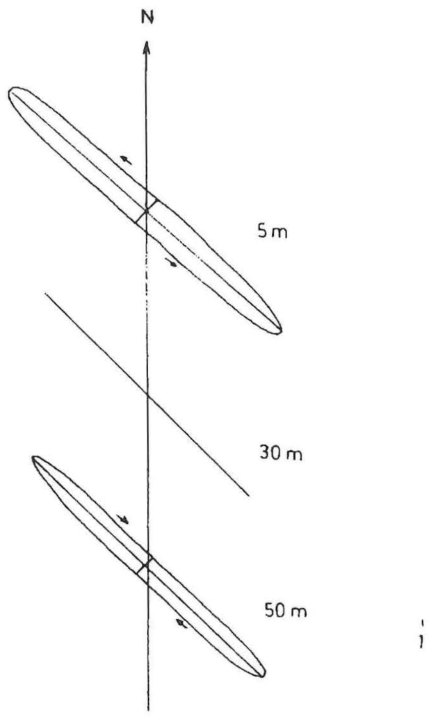

Fig. 4.21. Hodographs of the M2 tidal current component for the surface, intermediary and bottom layer in IKA.

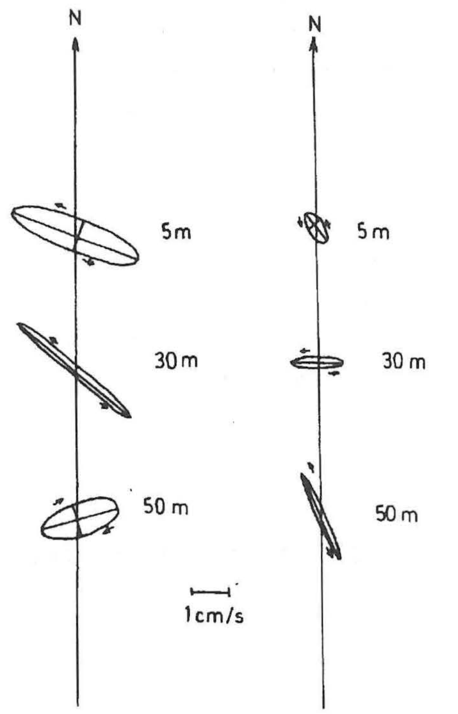

Fig. 4.23. Hodographs of the K1 + P1 tidal current components (left) and 01 component (right) for the surface, intermediary and bottom layer in IKA.

and the long period waves from the 12-hour and 24-hour oscillations. Shorter periods have been separated through the 4-hour moving average. Since the input values have been the hourly resultants, it was not possible to separate the periods shorter than two hours.The observed time interval is characterized by a relatively high shear of residual circulation in the current field. The values calculated as described in Ch.4.2. have been given for a comparison, so it can be noticed that this period is not typical. The mean circulation can be considered as thermohaline circulation, and it could be considered as baroclinic due to unequal heating and salinity changes in different layers. As expected, the most important oscillation periods are the 12 and 24-hour periods, because they include both tidal and inertial oscillations. Including the inertial oscillations, these fluctuations are also of a baroclinic character. Long period oscillations generated by the atmosphere are naturally baroclinic. The short period oscillations are not prominent.

Table. 4.9. The circulation kinetic energy 10^{-4} m^2 s^{-2} in the IKA field for the period Aug. 10th - Oct. 17th 1979.

Sea layer	Surf.	Interm.	Bott.
Total circulation kinetic energy	179	70	79
Kinetic energy of the mean (residual) circulation	120	15	9
Kinetic energy of long period oscil. (several days)	43	11	19
Kinetic energy of shorter period oscil. (more than 2h)	71	27	21
	8	4	3
Total circulation kinetic energy (as in Ch. 4.2.)	291	74	59
Kinetic energy of the mean (residual) circulation (Ch.4.2.)	120	15	7
Fluctuations kinetic energy (Ch.4.2.)	169	59	52

4.6. DRIFT-CARDS EXPERIMENT

The experiment purpose was to study water transport at the sea surface. It was planned to launch the cards from the research platforms every five days, but since the platforms changed their position or had a periodic repairing, it was not performed continually.

The number of drift cards recovered is much higher in the warm part of the year than in the cold one (Fig. 4.24.) probably because there are more people in summer than in winter. We have recovered almost no cards south of Istra on the eastern side of the Adriatic. That area has not been taken into analysis as it became obvious that the surface transport from

Table 4.10. The number of launched (L) cards from the fields IVANA (IV) and IKA (IK) for each month and the number of found cards (F), regardless of the date when they were found.

		1979		1980		1981		1982		1983		1984		1985		1986	
		L	F	L	F	L	F	L	F	L	F	L	F	L	F	L	F
Jan.	IV							150	10								
	IK			600	51									400	37		
Feb.	IV							300	37					50	3		
	IK													150	16		
Mar.	IV							300	114								
	IK			275	43									150	25	150	26
Apr.	IV							300	123			50	5	150	27		
	IK			100	7	100	26							150	28	150	40
May	IV							300	108			150	58	200	96		
	IK					250	72							200	97		
Jun.	IV							300	106			200	37				
	IK					200	59	100	31					200	59		
Jul.	IV					100	42										
	IK					200	42	200	82					50	8		
Aug.	IV											200	58			50	8
	IK	250	35			200	77	300	52					300	107		
Sep.	IV													100	36		
	IK	200	13			200	24	350	38			100	36	150	60		
Oct.	IV													150	15		
	IK	100	9			200	35	300	30			150	16	100	16		
Nov.	IV					250	30							100	4		
	IK					50	6	150	12			150	10				
Dec.	IV					100	6							50	3		
	IK	250	8									50	7				
Total	IV	-		-		450	78	1750	498	-		600	158	750	184	50	8
	IK	800	65	975	101	1400	341	1400	245	-		450	69	850	448	300	66

IVANA: total launched cards 3600, total found cards 926 (25.7%)
IKA: total launched cards 7175, total found cards 1335 (18.6&%)

the north Adriatic is not directed to the middle and south part of the east coast. This is also in accordance with the direction of residual flow in both fields (Fig. 4.5.).

To get an insight into the routes of the cards, the coast has been divided into equal sections, and the percentage of the found cards in each sector has been registered for both fields together (Fig. 4.25.). The highest number of cards has been found on the west coast of Istra and in the area from Ravenna to Pesaro. Then follows the section around Venezia, the estuary of the Po and around Ancona. This shows that the surface transport

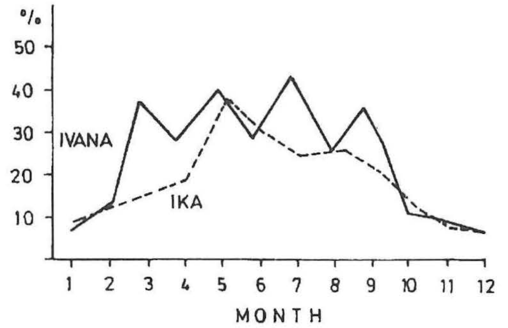

Fig. 4.24. Percentage of the found drift-cards for all months, out of the total number of found cards for the entire period.

from the middle part of the north Adriatic is directed towards the west coast of Istra and the Italian coast from Venezia to Ancona. The particular characteristics of the IVANA and IKA areas are shown in Fig. 4.26.

The wind on both fields has similar characteristics, so it cannot influence, to a higher extent, the differences in the transport of the cards from IVANA and IKA. A higher number of cards from the field IVANA has been found in the northern areas, while the ones from IKA in the southern areas. This is also in accor-

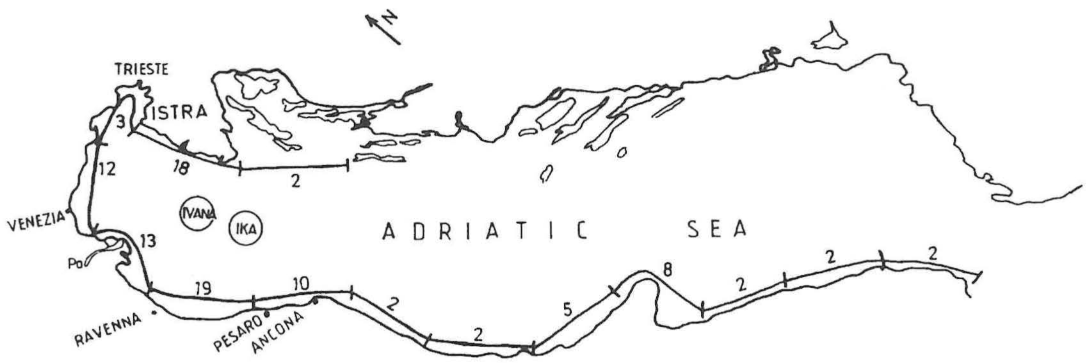

Fig. 4.25. Distribution of the found drift-cards on the coast. Figures indicate the percentage of the found cards for coast sectors.

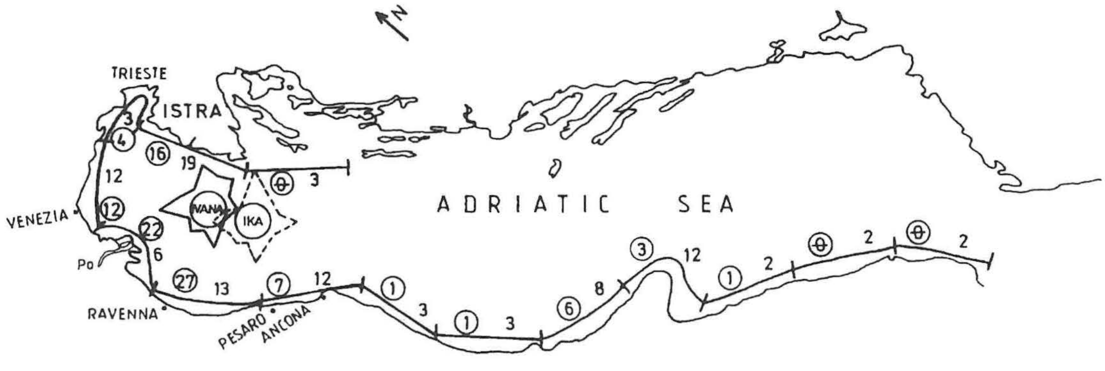

Fig. 4.26. Distribution of the found drift-cards in percentage according to the sectors on the coast, and the fields IVANA and IKA. Circled figures refer to the IVANA field. Wind roses for the fields IVANA and IKA have been given according the Fig. 2.6.

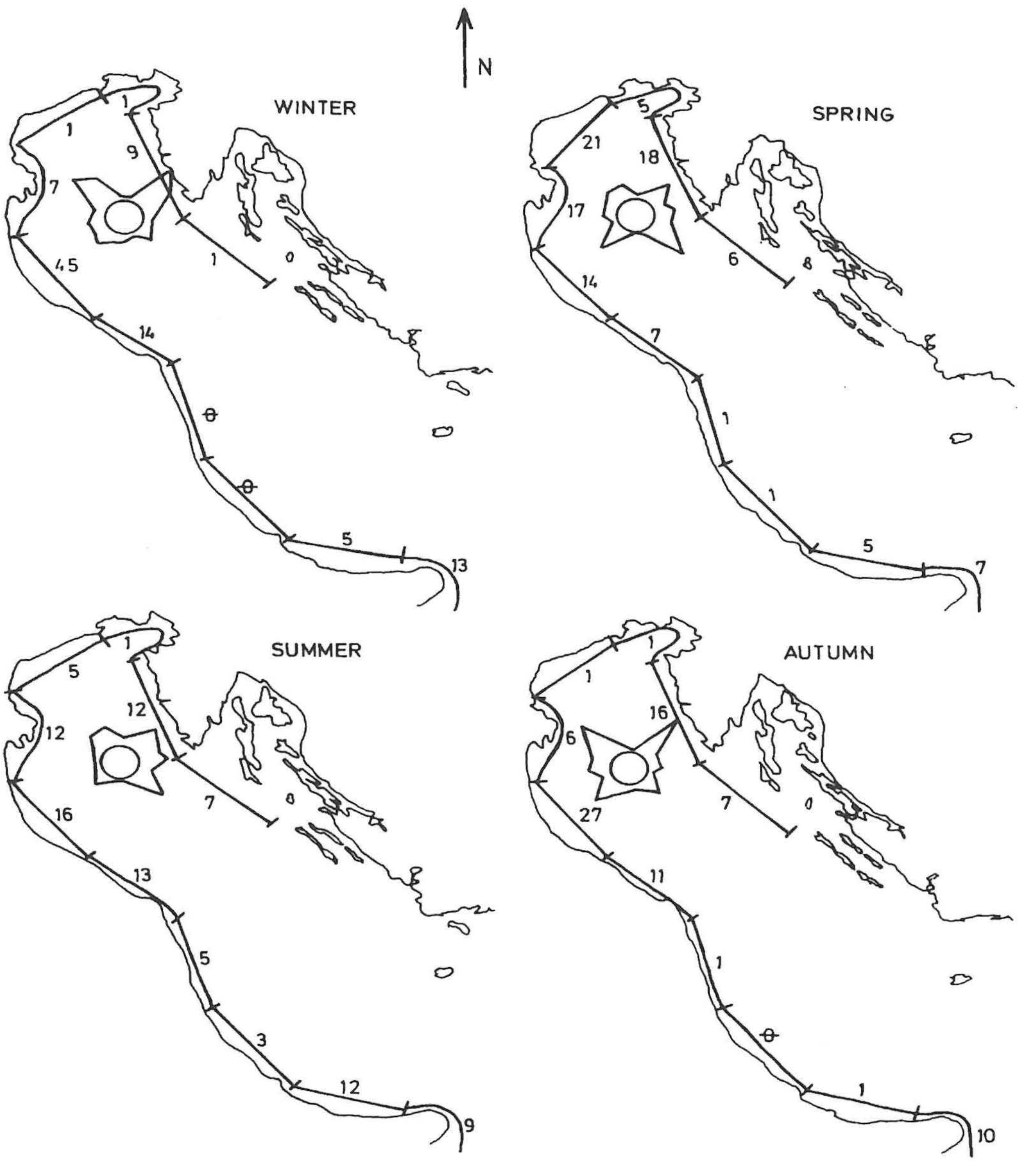

Fig. 4.27 Seasonal distribution of the found drift-cards from the IVANA and IKA field. Figures indicate the percentage of the total number of the found cards from both fields. Current roses have been given only for the IVANA field (after Fig. 2.7.), for the purpose of clearness.

dance with the directions of residual flow in the surface layer in both fields. The number of the found cards according to the seasons (Fig. 4.27.) also shows the essential influence of wind to their motion. In winter, with the strong Bora (NE wind), the highest number of cards has been found to the south-west of the fields of IVANA and IKA. A rather strong Bora also appears in autumn, but to a smaller extent, resulting in corresponding number of the cards found. A strengthened south-west wind in spring and autumn goes along with higher number of the found cards at the west coast of Istra (north-east of IVANA and IKA). Intensified SE wind (Scirocco) in spring produce higher number of the found cards in the nort-west Adriatic coast - the area of Venezia. All the findings prove that a strong wind is the essential factor in the transport of the cards, and the transport of dirt on the sea surface as well. In the next paper the influence of the Bora (NE) and the Scirocco (SE) winds on the circulation has been investigated. The directions of the transported cards influenced by the two winds is in accordance with the surface circulation generated by these winds (Figs 5.3a and 5.6a).

4.7. CONCLUSIONS

The residual flow for the entire period of measurements in the field IVANA has a low speed and small changes of direction in different layers: the north direction in the surface and the intermediary layers, and the north-east in the bottom layer. In the field IKA the residual flow is faster and it is W-oriented in all the layers. Basically, the residual flow function as one-layer system.

In the field IVANA the residual direction changes during the year. This prominent seasonal change of the direction follows the seasonal change of geostrophic circulation in the Middle Adriatic. In the field IKA the west direction is permanent throughout the year, which is also in accordance with the permanent west geostrophic current in that area. Therefore the seasonal residual flow practically corresponds to the geostrophic circulation.

The low kinetic energy of the mean current compared to the kinetic energy of fluctuations, especially in the bottom layer, shows that the oscillations are dominant in the current field. The highest kinetic energies of the mean current in both fields appear between August and November, with the simultaneous increase of the shear of the north and west current components.

The high values of the fluctuations kinetic energy are present in the field IVANA in warm period, the maximum being in the surface layer in June, appearing later at deeper layers. The elevated values appear at the same time in the field IKA, and in both fields they are connected to the strengthening of the east current component. The present assumption is that it is the influence of inertial oscillations, appearing at the open sea during the summer stratification.

Very high values of the fluctuations kinetic energy are present in IKA in the surface layer in the period between November and December, all current components also being of an outstanding maximum. It is assumed that they are influenced by long period oscillations, connected to passage of the synoptic disturbances in autumn and winter.

The residual directions are at the same time the most frequent: in IVANA northern at the surface, in IKA western. Equally frequent direction in IVANA is north-west. In lower layers the frequent directions are also NW and SE, referring to tidal currents. Alternative shear of the N and S directions display the seasonal changes in the frequency in IVANA in all layers: the former being more frequent in winter, the latter in spring and summer. In IKA the western direction appears most frequently throughout the year.

The currents in IVANA are generally of lower speed, compared to IKA. The mean scalar speed in the surface layer in IVANA is 12.5 cm s^{-1}, in IKA 12.8 cm s^{-1}. The corresponding maximum speeds are 70.1 cm s^{-1} and 88.0 cm s^{-1}. In deeper layers the speeds are lower, as well as the differences between the fields. Nevertheless, higher speeds classes in all the layers are more frequent in IKA.

In IVANA the scalar speed in all layers is higher than in IKA only in summer, which may be connected to the appearance of the inertial oscillations. The long period oscillations can be connected to the high scalar speed in IKA in autumn and comparatively high in winter.

The seasonal variations in the distribution of speeds by class intervals are most outstanding in the surface layer. In both fields the lowest speeds are most frequent in winter, and the highest speeds in summer.

In IVANA the most frequent directions

are not of highest speeds, as those occur with the W and SE directions. In IKA the highest speed, as a rule, is connected to the most frequent direction (W). In general, in both fields the higher class speeds are connected to the W and NW directions, the lower class speeds being connected to the directions of N, NE, E and SE.

The tidal current directions (NW and SE) in the surface layer are of lower speeds than other directions, while in the bottom layer they appear with the highest speeds. The similar relationship can be noticed for the north direction.

The periods of oscillations in the current field range from several hours to several days. During the summer marked vertical stratification, the highest energies on both fields have the oscillations of the inertial period (17h), which appear after sudden changes of the wind. They have clear rotational anticyclonic motion. The inertial oscillations are most outstanding in the surface layer, but are also present in the intermediary and bottom layer. They probably reach the maximum speeds up to 50 cm s^{-1}.

Of somewhat lower energy are the several days oscillations, which are connected to the changes of wind on the synoptic scale. Such oscillations are typical for the IKA field in autumn and winter, being mostly of E - W directions, that is, parallel to the isobaths.

The tidal currents have the periods of 12 and 24 hours, but the 12-hour oscillations are, in general, of higher energy. As a rule, they have the cyclonic rotation in the surface layer. The tidal current speeds are low- about 5 cm s^{-1}. The speeds do not change with the depth. The circulation caused by the tides is polarized in the direction of the coast (NW - SE) and, in general, is cyclonic.

The circulation at the very surface has been studied with the use of drift-cards. The surface transport from the fields IVANA and IKA is directed mostly towards the west coast of Istra and the Italian coast from Venezia to Ancona. A higher number of cards from IVANA has been found in the north sectors, while the cards from IKA have been found in greater number in the south coastal sectors. Wind is an essential factor for the transport of cards: in winter, with the strong Bora (NE wind), the main transport is directed towards the southwest from the gas fields, a strong south-west wind in spring and summer directs the transport towards the coast of Istra. A strong Scirocco (SE wind) intensify the transport towards Venezia. There is no transport towards the east coast to the south of Istra.

4.8. REFERENCES

BONE, M. 1986. On the profile of tidal currents in the northern Adriatic, Acta Adriat., 27 (1-2): 5-14.

BONE M. 1988: Kooscilacija Virskog mora pod utjecajem atmosfere i morskih mijena u Jadranu. Doktorska disertacija. Prirodno-matematički fakultet Univerziteta u Beogradu. 144 pp.

BRANA J. and V. KRAJCAR, 1995. General circulation of the northern Adriatic Sea - Results of long-term measurements. Estuarine, Coastal and Shelf Science 40:421-434.

BULJAN, M. 1964. Ocjena produktivnosti Jadrana dobivena na temelju njegovih hidrografskih svojstava. Acta Adriat., 11 (4): 34-65.

DEFANT, A. 1961. Physical oceanography. Vol. II. Pergamon Press, New York - Oxford -London - Paris, 598 pp.

GAČIĆ, M. 1980. Some characteristics of the response of the Adriatic sea coastal region to the atmospheric forcing. Acta Adriat., 21 (2): 239-254.

GAČIĆ, M. 1983. Dugoperiodične oscilacije u strujnom polju u Jadranu. Doktorska disertacija. Univerzitet u Beogradu, 102 pp.

GAČIĆ, M. and Z. VUČAK, 1982. Note on inertial oscillations in the North Adriatic. Bilj.-Notes Inst. Oceanogr. Ribar. Split, 46: 7 pp.

GONELLA, J. 1972. A rotary-component method for analyzing meteorological and oceanographic vector time series. Deep-Sea Res., 19(12): 833-846.

MOSETTI, F. e A. LAVENIA, 1969. Ricerche oceanografiche in Adriatico nel periodo 1966-1968. Boll. geof. teor. appl. 11 (43-44): 1-28.

STRAVISI, F. 1973. Analysis of a storm surge in the Adriatic Sea by means of a two-dimensional linear model. Accad. Naz. Lincei, Rend. VIII 54 (2): 243-260.

TEE, K.T. 1979. The structure of three-dimensional tide generating currents, Part I: Oscillations currents. Phys. Ocean., 9: 930-944.

VUČAK, Z. i A. SMIRČIĆ, 1983. Usporedba podataka strujomjernih stanica na OC poligonu PANON u periodu Alpex-med-alpex programa. Dinamika vjetra i strujanja u sjevernom Jadranu - Alpex rezultati. Savezni Hidrometeorološki zavod, Beograd, Institut za oceanografiju i ribarstvo, Split. pp. 6.

ZORE, M. 1956. On gradient currents in the Adriatic Sea, Acta Adriat. 8(6): 1-38.

ZORE-ARMANDA, M. 1966. The system of currents found at a control station in the middle Adriatic. Acta Adriat., 10(11): 20 pp.

ZORE-ARMANDA, M. and M. GAČIĆ, 1987. Effect of Bora on the circulation of the North Adriatic. Annales Geophysicae 5B (1): 93-102

ZORE-ARMANDA, M. and Z. VUČAK, 1984. Some properties of the residual circulation in the northern Adriatic. Acta Adriat. 25(1/2): 101-117.

Ekološka studija plinskih polja u sjevernom Jadranu

Strujanje

Mira ZORE ARMANDA+, Mario BONE+, Vlado DADIĆ+, Miroslav GAČIĆ+*, Vedrana KOVAČEVIĆ++ i Zoran VUČAK++

+*Institut za oceanografiju i ribarstvo, Split, Hrvatska*

++*Državni hidrografski Institut, Split, Hrvatska*

**Osservatorio Geofisico Sperimentale, Trieste, Italija*

KRATKI SADRŽAJ

U vremenu od 1978 -1986 mjerile su se struje s istraživačkh platformi na poljima IVANA i IKA. Prikupljeno je 168 065 strujomjernih podataka na lokaciji IVANA i 284 570 na lokaciji IKA. Za sve podatke provedena je detaljna statistička analiza. Osim toga sa obje lokacije su bacane drift kartice za mjerenja površinskih struja. Ukupno je bačeno sa lokacije IVANA 3600 a sa lokacije IKA 7175 kartica od čega je nađeno cca. 20% kartica. Strujno polje je na obje lokacije iscrpno opisano posebno s aspekta udjela raznih tipova strujanja u strujnom polju.

Table 4.A.1 Processed current data of the field IVANA for the whole period of measurement, from 24. May 1978 through 24. March 1986. Speeds are in cm s^{-1}, and directions are in degrees.

			Vector velocity		Scalar speed				N component				E component				Kinetic energy (10^{-4} m^2 s^{-2})		
	IVANA r:44°35'-44°47' l:13°07'-13°25'	Total number of data	Direction	.Velocity	Mean	St.dev.	Min.	Max.	Mean	St.dev	Min.	Max.	Mean	St.dev	Min.	Max.	Fluct.	Mean	Total
SURFACE LAYER (5m)	Whole period	73248	339 N	1.0	12.5	8.4	0.0	70.1	0.9	10.4	-48.0	60.1	-0.3	10.9	-59.0	69.5	113.2	0.5	113.7
	Winter	27132	10 N	2.7	9.7	5.6	0.0	37.1	2.6	8.1	-31.9	30.3	0.5	7.3	-26.7	34.2	59.3	3.5	62.8
	Spring	18941	99 E	0.7	13.9	10.1	1.0	70.1	-0.1	11.9	-49.8	69.5	0.7	12.3	-48.0	60.1	146.7	0.3	146.6
	Summer	11396	188 S	3.5	17.3	10.3	1.5	63.1	-3.4	12.3	-59.0	60.0	-0.5	15.5	-43.0	53.4	196.7	6.1	202.8
	Autumn	15779	308 NW	3.7	12.2	6.9	1.5	53.6	2.3	9.4	-53.6	32.8	-2.9	9.7	-35.9	35.7	90.6	6.8	97.4
INTERM-EDIATE LAYER (20m)	Whole period	47145	343 N	1.8	10.1	6.9	1.5	58.0	1.8	9.2	-52.6	43.2	-0.5	7.8	-41.5	32.8	73.0	1.7	74.7
	Winter	17383	9 N	3.4	8.9	5.5	1.5	35.7	3.4	7.8	-29.2	20.7	0.5	6.0	-21.0	31.2	48.6	5.8	54.4
	Spring	13882	341 N	0.8	8.1	5.8	1.5	34.0	0.8	7.3	-28.6	28.4	-0.3	6.7	-27.3	28.2	49.0	0.3	49.4
	Summer	7500	161 S	0.7	15.0	9.5	1.5	58.0	-0.7	13.0	-41.5	32.8	0.2	12.0	-52.6	43.2	156.6	0.3	156.9
	Autumn	8380	301 NW	4.5	11.4	6.3	1.5	43.2	2.3	10.0	-29.1	31.7	-3.9	7.1	-27.0	35.9	75.2	10.1	85.3
BOTTOM LAYER (40m)	Whole period	53672	60 NE	0.4	6.1	4.1	1.0	37.0	0.2	5.7	-31.5	24.2	0.4	4.7	-27.5	27.6	27.1	0.1	27.2
	Winter	25234	22 N	1.5	5.6	3.7	1.0	35.4	1.4	5.1	-27.5	17.1	0.5	4.2	-13.7	24.2	21.8	1.1	22.9
	Spring	8395	286 W	0.4	5.6	3.7	1.0	26.0	0.1	5.3	-24.4	14.8	-0.3	4.0	-17.3	19.9	22.2	0.1	22.3
	Summer	7445	167 S	1.3	8.0	5.3	1.5	37.0	-1.3	7.5	-25.4	27.6	0.3	5.8	-31.5	24.0	45.0	0.9	45.9
	Autumn	12598	150 SE	1.2	6.5	3.8	1.5	31.5	-1.1	5.3	-19.0	27.6	0.6	5.1	-23.3	19.9	27.3	0.7	28.0

Table 4.A.2. Processed current date of the field IKA for the whole period from 10 August1979 throught 13 May 1986.

			Vector velocity		Scalar speed				N component				E component				Kinetic energy $(10^{4}\ m^{2}\ s^{2})$		
	IKA r:44°17'-44°32' l:13°13'-13°38'	Total number of data	Direction	.Velocity	Mean	St.dev.	Min.	Max	Mean	St.dev	Min	Max	Mean	St.dev	Min	Max	Fluct.	Mean	Total
SURFACE LAYER (5m)	Whole period	102677	266 W	5.9	17.8	15.4	1.0	94.2	-0.4	14.4	-84.8	84.0	-5.9	17.6	-94.2	79.9	259.7	17.4	277.2
	Winter	17425	260 W	5.9	16.3	14.4	1.5	80.0	-0.1	13.4	-77.0	73.0	-5.8	16.0	-79.7	72.4	218.8	17.6	236.4
	Spring	19677	274 W	4.8	14.9	12.2	1.0	94.2	0.4	12.5	-94.2	79.9	-4.8	13.8	-84.8	70.3	173.8	11.7	185.5
	Summer	32458	260 W	6.8	16.4	10.4	1.5	66.0	-1.2	10.9	-65.7	52.5	-6.7	14.5	-44.2	56.5	165.1	22.9	188.0
	Autumn	33177	272 W	5.8	21.8	20.1	1.0	88.0	-0.2	18.4	-85.0	78.7	-5.8	22.6	-78.8	84.0	423.7	16.8	440.5
INTERM-EDIATE LAYER (30m)	Whole period	84927	260 W	2.8	9.8	6.2	1.0	56.0	-0.5	8.0	-53.2	34.8	-2.8	7.9	-48.5	34.0	63.6	4.1	67.7
	Winter	16685	82 E	0.4	9.1	5.2	1.5	32.0	0.1	7.1	-28.7	24.3	0.4	7.7	-26.6	27.0	54.9	0.1	55.0
	Spring	12475	266 W	3.0	9.0	4.7	1.0	33.0	-0.2	7.2	-30.9	19.7	-3.0	6.6	-25.2	26.4	47.4	4.6	52.0
	Summer	31346	262 W	2.5	9.2	6.0	1.0	53.0	-0.3	7.9	-45.2	26.5	-2.4	7.3	-31.9	34.8	57.5	3.0	60.6
	Autumn	24421	258 W	5.5	11.6	7.3	1.5	56.0	-1.2	9.2	-48.5	34.0	-5.4	8.5	-53.2	31.0	78.4	15.1	93.5
BOTTOM LAYER (50m)	Whole period	96966	243 SW	2.1	7.5	5.0	1.0	46.0	-1.0	6.3	-40.4	33.7	-1.9	6.1	-45.8	30.4	38.2	2.2	40.4
	Winter	19890	243 SW	3.5	7.9	4.8	1.5	38.0	-1.6	6.3	-36.5	16.5	-3.1	5.8	-36.7	21.7	36.7	6.0	42.7
	Spring	17416	243 SW	1.9	7.6	4.7	1.5	34.8	-0.9	6.2	-29.3	30.4	-1.7	6.2	-30.2	33.7	38.4	1.8	40.1
	Summer	26242	263 W	0.6	6.7	4.4	1.0	41.0	-0.1	5.5	-37.0	25.7	-0.6	5.8	-40.4	25.6	32.0	0.2	32.2
	Autumn	33418	240 SW	2.6	7.8	5.5	1.0	46.0	-1.3	6.7	-45.8	28.7	-2.2	6.3	-34.8	25.6	42.4	3.3	45.7

With no 5 doubtful series

(5m)	Whole period	96823	265 W	4.4	15.0	10.0	1.0	94.2	-0.4	10.5	-84.8	70.3	-4.4	13.9	-94.2	79.9	152.6	9.8	162.4
	Winter	16317	262 W	4.1	13.0	6.7	1.5	44.0	-0.6	8.5	-43.3	38.4	-4.1	11.2	-32.8	26.0	98.6	8.6	107.2
	Autumn	28371	270 W	1.7	14.5	9.3	1.0	66.0	0.0	9.6	-63.0	49.7	-1.7	14.3	-47.9	36.4	147.3	1.4	148.7

Table 4.A.3. Processed current data at the field IVANA for the whole period of measurement, from 24 May 1978 throught 24 March 1986. Speeds are in cm s^{-1}, directions are in degrees.

		Vector velocity		Scalar speed				N component				E component				Kinetic energy $(10^4\ m^2 s^2)$		
Layer	Month	Direction	Velocity	Mean	St. dev.	Min.	Max.	Mean	St. dev.	Min.	Max.	Mean	St. dev.	Min.	Max.	Fluct.	Mean	Total
Surface layer (5m)	1	329.2 NW	1.5	6.9	4.5	0.0	28.0	1.3	6.0	-23.2	20.8	-0.8	5.5	-21.7	19.8	32.9	1.2	34.0
	2	9.8 N	3.1	10.8	5.3	0.0	37.1	3.0	8.7	-31.9	30.3	0.5	7.7	-25.1	34.2	68.1	4.8	72.9
	3	22.6 NE	3.4	10.7	5.8	1.5	30.0	3.2	8.6	-29.4	24.2	1.3	8.0	-26.7	29.5	68.6	5.9	74.4
	4	304.6 NW	0.7	9.0	5.3	1.5	34.0	0.4	8.0	-30.5	20.7	-0.5	6.7	-33.7	31.5	54.5	0.2	54.7
	5	259.9 W	0.7	14.2	8.8	1.5	50.8	-0.1	12.4	-45.8	42.4	-0.7	11.3	-48.0	44.6	139.9	0.3	140.1
	6	100.5 E	3.0	18.1	12.1	1.0	70.1	-0.5	14.3	-49.8	69.5	2.9	16.2	-47.8	60.1	233.4	4.5	237.9
	7	117.5 SE	3.7	18.5	10.5	1.5	63.1	-1.7	13.4	-38.5	60.0	3.3	16.1	-39.3	53.4	220.3	6.8	227.1
	8	190.9 S	5.6	16.5	9.0	1.5	48.3	-5.5	11.9	-45.5	44.9	-1.1	13.4	-43.0	38.9	161.4	15.6	177.1
	9	267.3 W	10.8	16.5	13.8	1.5	59.0	-0.5	8.1	-59.0	11.8	-10.8	16.8	-37.3	36.0	173.0	58.0	231.0
	10	309.2 NW	9.4	16.1	4.9	6.5	29.5	5.9	12.3	-22.4	20.3	-7.3	6.6	-28.1	27.5	97.5	44.0	141.5
	11	280.5 W	5.5	13.2	7.5	1.5	53.6	1.0	9.7	-53.6	22.5	-5.4	10.3	-35.9	29.8	100.2	15.4	115.6
	12	3.9 N	3.4	10.6	5.9	1.5	35.9	3.3	8.5	-33.9	32.8	0.2	8.0	-23.9	35.7	68.3	5.6	73.9
Interme-diate layer (20m)	1	350.9 N	2.7	7.9	5.1	2.0	31.0	2.7	7.7	-17.7	13.9	-0.4	4.8	-21.0	26.8	40.8	3.6	44.4
	2	358.1 N	4.4	9.5	5.5	2.0	35.7	4.4	7.6	-29.9	18.2	-0.1	6.7	-15.8	31.2	51.1	9.6	60.7
	3	18.9 N	3.3	8.9	5.5	1.5	29.0	3.1	7.9	-23.9	20.7	1.1	6.0	-19.0	29.0	49.1	5.5	54.6
	4	19.7 N	0.6	6.9	4.8	1.5	29.0	0.5	6.1	-23.5	28.4	0.2	5.7	-24.4	28.0	34.8	0.2	35.0
	5	292.1 W	1.4	8.4	6.1	1.5	30.0	0.5	7.7	-25.9	23.8	-1.3	6.8	-25.2	24.9	52.9	1.0	53.9
	6	16.2 N	2.1	10.6	6.7	3.0	34.0	2.0	9.2	-28.6	27.0	0.6	8.3	-27.3	28.2	76.8	2.1	79.0
	7	90.3 E	4.2	12.2	7.4	1.5	40.7	0.0	11.2	-18.6	28.3	4.2	7.8	-30.2	31.9	93.6	8.9	102.5
	8	124.9 SE	1.9	15.5	9.3	1.5	58.0	-1.1	14.0	-40.1	32.8	1.6	11.3	-52.6	43.2	161.2	1.9	163.1
	9	275.1 W	11.9	14.6	11.6	1.5	44.0	1.1	7.5	-41.5	7.6	-11.9	12.1	-19.9	26.8	101.8	71.2	173.0
	10	315.1 NW	15.2	19.0	9.8	1.8	43.2	10.8	13.5	-25.0	4.9	-10.8	6.8	-20.3	35.9	113.5	116.0	229.5
	11	281.3 W	4.0	10.9	5.2	1.5	28.0	0.8	9.0	-25.7	20.7	-3.9	7.0	-23.2	27.0	65.4	7.8	73.2
	12	322.9 NW	3.9	10.7	6.0	1.5	35.0	3.1	9.7	-29.1	31.7	-2.4	6.4	-27.0	32.9	67.5	7.6	75.1
Bottom layer (40m)	1	133.5 SE	0.9	5.1	3.1	1.5	18.9	-0.6	4.3	-14.4	17.1	0.7	4.1	-12.8	15.0	17.6	0.4	18.1
	2	355.2 N	2.3	5.5	4.4	1.0	35.4	2.3	5.0	-27.5	12.2	-0.2	4.4	-13.7	24.2	22.0	2.6	24.6
	3	25.2 N	2.3	6.1	3.6	1.0	21.1	2.1	5.2	-18.1	15.1	1.0	4.1	-11.5	20.9	22.3	2.7	25.1
	4	295.4 NW	0.6	5.1	3.2	1.0	20.0	0.2	4.9	-12.3	12.6	-0.5	3.4	-17.3	13.9	17.8	0.2	18.0
	5	217.3 SW	0.4	6.9	4.0	1.5	23.0	-0.3	6.3	-14.8	14.6	-0.2	4.9	-15.6	19.9	31.5	0.1	31.6
	6	325.5 NW	0.2	5.1	4.0	2.0	26.0	0.2	5.0	-24.4	14.8	-0.1	4.2	-15.0	16.9	21.2	0.0	21.2
	7	122.6 SE	3.2	7.4	4.5	1.5	21.1	-1.7	6.6	-6.9	15.7	2.7	4.6	-18.3	13.4	32.3	5.0	37.3
	8	148.1 SE	1.3	7.9	5.3	1.5	37.0	-1.1	7.7	-17.4	27.6	0.7	5.5	-31.2	24.0	44.2	0.9	45.1
	9	249.0 W	5.1	9.2	5.9	1.5	32.0	-1.8	7.4	-25.4	7.2	-4.7	6.3	-31.5	13.8	47.0	12.8	59.8
	10																	
	11	120.5 SE	2.1	6.7	4.0	1.5	31.5	-1.1	5.3	-19.0	27.6	1.8	5.3	-18.7	19.9	28.2	2.3	30.5
	12	197.4 S	1.1	6.3	3.6	1.5	23.3	-1.0	5.4	-17.9	14.8	-0.3	4.7	-23.3	17.9	25.7	0.6	26.3

Table 4.A.4. Processed current data at the field IKA for the whole period from 10 August 1979. throught 13 May 1986. Speeds are in cm s^{-1}, directions are in degrees.

		Vector velocity		Scalar speed				N component				E component				Kinetic energy $(10^{4}\ m^{2}\ s^{2})$		
Layer	Month	Direction	Velocity	Mean	St. dev.	Min.	Max.	Mean	St. dev.	Min.	Max.	Mean	St. dev.	Min.	Max.	Fluct.	Mean	Total
Surface layer (5m)	1	259.8 W	5.3	22.6	20.2	1.5	80.8	-0.9	19.1	-77.0	73.0	-5.2	22.8	-79.7	72.4	444.0	14.0	457.9
	2	256.7 W	6.3	11.6	6.0	1.5	31.0	-1.5	7.8	-31.0	24.8	-6.1	8.3	-25.1	24.6	65.3	19.9	85.3
	3	264.0 W	6.4	13.6	7.5	2.1	38.2	-0.7	8.7	-38.2	23.2	-6.3	11.3	-28.0	25.6	101.1	20.3	121.4
	4	303.6 NW	3.5	12.4	5.2	2.6	33.1	1.9	8.7	-32.0	27.4	-2.9	9.6	-27.3	27.4	84.2	6.1	90.3
	5	274.8 W	4.9	11.1	6.0	1.0	37.3	0.4	7.6	-31.9	34.3	-4.9	8.8	-30.6	24.3	67.4	12.2	79.6
	6	262.3 W	6.1	21.3	17.5	1.5	94.2	-0.8	18.1	-94.2	79.9	-6.1	19.9	-84.8	70.3	361.5	18.7	380.2
	7	232.7 SW	3.5	13.0	7.9	1.5	51.0	-2.1	9.3	-50.8	33.1	-2.8	11.5	-32.0	34.9	109.6	6.3	115.9
	8	262.7 W	7.2	15.1	9.6	2.0	66.0	-0.9	10.4	-65.7	40.0	-7.2	12.6	-44.2	46.8	133.4	26.0	159.4
	9	265.2 W	8.7	19.2	11.4	1.5	63.1	-0.7	12.1	-61.1	52.5	-8.7	16.7	-43.3	56.5	211.8	37.8	249.6
	10	258.6 W	5.0	17.0	9.9	1.5	66.0	-1.0	10.8	-63.0	49.7	-4.9	15.6	-47.9	31.5	180.9	12.7	193.6
	11	297.8 NW	9.1	25.9	24.3	1.5	86.0	4.3	21.1	-85.0	73.9	-8.1	27.1	-75.3	84.0	587.8	41.7	629.5
	12	257.7 W	5.4	26.2	26.1	1.0	88.0	-1.2	24.3	-84.7	78.7	-5.3	27.3	-78.8	73.9	666.8	14.8	681.6
Interme-diate layer (30m)	1	253.9 W	2.9	9.7	5.0	1.5	32.0	-0.8	7.0	-28.7	15.8	-2.8	7.8	-26.6	16.9	55.5	4.2	59.6
	2	90.4 E	2.0	8.4	5.0	1.5	28.1	0.0	7.0	17.2	22.6	2.0	6.5	-24.1	27.0	45.9	2.1	48.0
	3	60.7 NE	2.0	9.2	5.6	1.5	27.5	1.0	7.2	-19.7	24.3	1.7	7.8	-17.4	23.3	55.8	2.0	57.8
	4	269.6 W	3.6	9.0	4.5	1.5	24.2	0.0	6.9	-23.9	16.0	-3.6	6.4	-23.4	20.0	44.2	6.6	50.7
	5	261.6 W	3.8	8.9	4.6	1.0	23.0	-0.5	6.9	-20.8	17.9	-3.7	6.2	-20.8	18.2	43.0	7.1	50.2
	6	266.4 W	1.7	9.2	5.0	1.0	33.0	-0.1	7.7	-30.9	19.7	-1.7	6.9	-25.2	26.4	53.4	1.5	54.9
	7	224.8 SW	0.8	8.3	4.9	1.5	30.6	-0.6	7.3	-21.9	26.3	-0.6	6.3	-26.9	24.4	46.4	0.3	46.7
	8	260.6 W	1.6	7.9	4.9	1.0	29.0	-0.3	6.6	-27.9	20.8	-1.6	6.3	-24.2	25.6	42.0	1.3	43.3
	9	266.6 W	4.2	10.7	7.0	1.5	53.0	-0.3	8.9	-45.2	26.5	-4.2	8.1	-31.9	34.8	72.4	9.0	81.4
	10	250.3 W	6.6	13.3	7.2	1.5	56.0	-2.2	10.0	-48.5	34.0	-6.2	9.3	-53.2	31.0	93.1	21.5	114.5
	11	287.0 W	5.4	11.5	7.5	1.5	40.0	1.6	9.4	-32.8	21.9	-5.2	8.3	-27.3	30.9	78.8	14.6	93.4
	12	253.4 W	4.3	8.7	6.3	1.5	36.5	-1.2	7.0	-31.5	20.3	-4.1	6.9	-26.5	28.2	48.0	9.2	57.2
Bottom layer (50m)	1	243.7 SW	4.2	7.8	4.9	1.5	38.0	-1.9	5.8	-36.5	12.6	-3.8	5.7	-36.7	15.5	33.0	9.0	42.0
	2	230.6 SW	3.6	7.6	4.3	1.5	23.0	-2.3	6.0	-21.8	16.5	-2.8	5.2	-22.9	18.9	31.6	6.4	38.0
	3	252.4 W	2.8	8.3	5.0	1.5	22.9	-0.9	6.9	-22.2	15.2	-2.7	6.2	-22.9	18.9	43.0	3.9	46.9
	4	244.2 SW	2.3	6.7	3.4	1.5	20.3	1.0	4.8	-18.8	12.1	-2.1	5.2	-18.6	14.0	25.3	2.8	28.0
	5	243.9 SW	2.5	7.5	4.0	1.5	24.0	-1.1	5.9	-22.7	18.2	-2.2	5.5	-18.4	15.4	32.8	3.0	35.8
	6	235.5 SW	0.9	8.6	5.9	1.5	34.8	-0.5	7.4	-29.3	30.4	-0.8	7.3	-30.2	33.7	53.9	0.4	54.3
	7	53.4 NE	0.1	6.1	3.9	1.5	27.0	0.1	5.2	-15.4	19.1	0.1	5.0	-20.7	19.1	26.2	0.0	26.2
	8	263.9 W	1.0	6.5	4.2	1.0	27.0	-0.1	5.4	-21.8	17.4	-1.0	5.5	-26.6	19.9	29.2	0.5	29.7
	9	260.0 W	0.9	7.1	4.8	1.0	41.0	-0.2	5.8	-37.0	25.7	-0.9	6.3	-40.4	25.6	36.6	0.4	37.0
	10	222.6 SW	2.1	8.1	5.3	1.5	46.0	-1.5	7.0	-45.8	28.7	-1.4	6.4	-32.9	23.9	44.9	2.1	47.0
	11	247.6 W	2.7	7.9	5.7	1.0	32.0	-1.0	7.0	-28.2	21.3	-2.5	6.1	-30.5	20.8	43.4	3.7	47.2
	12	249.7 W	3.5	7.2	5.7	1.5	38.0	-1.2	5.8	-32.2	21.9	-3.3	6.3	-34.8	25.6	36.3	6.0	42.3

Without 5 doubtful series

Surface layer (5m)	1	26.6 NE	0.3	14.0	6.3	1.5	44.0	0.3	8.9	-43.3	38.4	0.1	12.5	-32.8	26.0	117.9	0.0	117.9
	11	5.0 N	1.0	13.3	7.0	1.5	41.0	1.0	8.3	-40.0	32.4	0.1	12.5	-33.7	34.9	112.2	0.5	112.7
	12	72.6 E	4.4	9.8	7.7	1.0	37.0	1.3	6.9	-34.0	35.0	4.2	9.5	-30.5	36.4	68.6	9.7	78.3

Table 4.A.5. Direction and speed frequencies (%) at the field IVANA for the period from 24 May 1978 through 24 March 1986.

		SURFACE LAYER (5 m)									INTERMEDIATE LAYER (20 m)									BOTTOM LAYER (40 m)								
IVANA j=44°35'-44°47' l=13°07'-13°25'		N	NE	E	SE	S	SW	W	NW	speed freq. (%)	N	NE	E	SE	S	SW	W	NW	speed freq. (%)	N	NE	E	SE	S	SW	W	NW	speed freq. (%)
WHOLE PERIOD																												
Dir. frequency		17	10	12	13	11	9	11	17		21	9	10	16	10	7	9	18		18	8	10	22	11	5	7	18	
Mean speed		11.3	11.8	13.4	12.0	12.3	14.2	14.8	11.7		10.7	7.0	7.6	10.3	9.9	8.9	11.2	12.1		6.0	4.2	4.8	7.2	6.4	5.1	5.4	7.1	
	0-5	18	19	17	16	16	13	13	16	16	21	45	41	26	29	29	24	19	29	50	70	61	34	44	60	56	36	51
	5-10	31	30	27	32	28	23	24	33	28	30	32	33	30	29	32	25	25	30	35	26	33	44	39	32	31	40	35
	10-15	25	25	23	25	24	25	23	26	24	23	14	15	21	22	25	24	24	21	12	3	6	16	13	5	10	19	10
(cm s^{-1})	15-20	14	13	15	12	16	16	15	12	14	16	7	7	12	12	10	13	17	12	4	0	0	4	3	1	2	4	2
	20-25	6	5	7	6	9	11	10	7	8	7	2	2	5	4	3	8	9	5	0	0	0	1	1	1	1	1	1
	25-30	2	3	3	4	3	5	7	3	4	2	0	1	3	2	1	3	3	2	0	0	0	0	0	0	0	0	0
WINTER																												
Dir. frequency		23	12	13	10	8	5	7	18		29	13	13	15	6	4	4	13		23	10	12	20	6	3	5	17	
Mean speed		10.0	9.6	9.6	9.1	9.7	10.4	10.6	9.7		10.7	6.5	6.5	7.7	7.7	8.3	10.3	11.2		6.3	4.1	4.6	6.1	4.6	4.4	5.1	6.8	
	0-5	22	23	21	21	22	23	21	21	22	17	48	48	31	35	26	22	19	31	47	74	62	39	62	62	60	39	56
	5-10	31	35	35	38	34	27	31	38	34	32	32	35	39	34	40	29	29	34	34	21	32	49	35	35	28	40	34
	10-15	25	22	27	26	23	27	24	26	25	24	11	9	20	20	24	26	19	19	12	3	4	9	2	1	7	15	7
(cm s^{-1})	15-20	14	13	12	10	15	14	10	8	12	18	7	6	8	9	7	13	18	11	4	0	0	0	0	0	2	3	1
	20-25	5	4	3	2	4	5	7	4	4	6	0	0	0	0	1	7	10	3	0	0	0	0	0	0	0	1	0
	25-30	1	0	0	0	0	2	3	1	1	0	0	0	0	0	0	0	1	0	0	0	0	0	0	0	0	0	0
SPRING																												
Dir. frequency		13	9	11	15	14	9	11	14		16	7	9	18	10	6	9	21		17	6	6	18	15	6	7	21	
Mean speed		13.3	14.8	16.3	13.9	12.9	13.5	13.7	13.0		7.8	5.8	7.1	9.0	7.4	6.2	8.1	9.4		4.9	3.3	4.2	6.4	5.9	4.7	4.6	6.8	
	0-5	16	16	15	14	15	16	18	17	16	40	56	45	33	45	55	42	30	43	61	86	73	45	44	65	69	44	61
	5-10	27	24	18	25	26	30	28	27	26	28	25	29	27	24	22	24	28	26	29	11	16	30	43	29	22	31	26
	10-15	22	23	21	25	24	19	20	23	22	18	13	15	20	19	15	16	21	17	8	2	9	20	10	4	5	19	10
(cm s^{-1})	15-20	12	13	15	13	13	9	8	11	12	8	3	5	10	7	3	11	12	7	0	0	0	3	1	0	0	3	1
	20-25	8	5	9	7	11	8	7	8	8	3	1	1	5	3	2	4	5	3	0	0	0	0	0	0	0	0	0
	25-30	4	5	5	6	4	5	7	5	5	0	0	1	1	0	0	1	1	0	0	0	0	0	0	0	0	0	0
SUMMER																												
Dir. frequency		5	6	14	16	14	16	14	10		13	10	12	18	11	8	13	12		16	6	8	22	15	6	7	16	
Mean speed		15.2	15.5	20.2	15.7	15.5	16.9	19.6	18.3		16.3	10.0	11.6	18.2	16.2	11.7	15.9	16.0		6.4	4.2	4.8	10.7	8.9	7.7	7.2	8.3	
	0-5	11	10	5	9	8	6	6	8	8	10	21	16	6	12	17	11	15	13	44	64	63	17	23	45	36	24	40
	5-10	24	25	16	26	16	15	17	13	19	19	34	28	14	20	28	21	18	23	38	34	27	33	41	27	37	43	35
	10-15	19	24	15	18	23	25	17	22	20	19	24	30	20	21	22	18	17	21	11	0	6	27	22	12	17	24	15
(cm s^{-1})	15-20	20	16	17	14	23	19	16	15	17	15	12	11	20	15	17	14	15	15	4	0	0	13	7	4	5	6	5
	20-25	11	7	14	13	14	14	10	16	12	15	6	9	16	10	7	13	11	11	0	0	0	4	2	7	1	0	2
	25-30	4	6	9	8	6	8	11	10	8	11	0	3	10	7	4	10	8	7	0	0	0	1	1	1	0	0	0
AUTUMN																												
Dir. frequency		19	8	7	11	7	9	14	22		17	4	3	10	12	11	12	27		8	6	9	26	14	6	11	16	
Mean speed		11.4	11.5	9.9	9.6	11.2	15.3	16.0	11.7		11.3	6.6	5.5	9.8	10.6	10.0	11.1	14.7		5.6	5.2	5.6	7.5	7.0	4.7	5.3	7.2	
	0-5	13	17	23	18	14	7	5	10	13	12	39	48	17	13	15	13	4	20	52	49	47	28	39	61	54	29	45
	5-10	35	25	30	39	33	17	17	35	29	30	42	42	36	35	35	26	20	33	34	46	42	47	37	31	34	44	39
	10-15	26	33	24	28	25	28	27	28	27	29	12	7	28	28	33	37	31	26	10	3	8	19	17	5	10	22	12
	15-20	15	11	16	10	15	21	24	15	16	18	2	0	12	17	12	13	23	12	2	0	0	3	4	1	0	2	2
	20-25	5	5	3	2	7	16	12	6	7	7	1	0	3	4	1	8	11	4	0	0	0	0	0	0	0	0	0
	25-30	3	3	0	0	1	4	7	2	3	1	0	0	0	0	0	0	4	1	0	0	0	0	0	0	0	0	0

Table 4.A.6. Direction and speed frequencies (%) at the field IKA for the period from 10 August 1979 through 13 May 1986.

SURFACE LAYER (5 m)

IKA j=44°17'-44°32' l=13°13'-13°38'	N	NE	E	SE	S	SW	W	NW	speed freq. (%)
WHOLE PERIOD									
Dir. frequency	8	8	10	9	11	15	23	17	
Mean speed	14.0	14.8	15.9	16.01	15.1	18.8	21.7	18.9	
0-5	14	11	10	4	13	10	6	9	11
5-10	29	24	20	26	27	21	16	22	23
10-15	28	25	26	24	27	23	21	26	25
(cm s^{-1}) 15-20	13	16	17	13	13	14	16	15	15
20-25	6	12	13	9	8	10	12	9	10
25-30	3	5	7	4	4	6	8	5	5
WINTER									
Dir. frequency	6	5	9	9	10	15	22	20	
Mean speed	12.7	12.7	14.9	15.7	13.7	18.2	18.8	16.5	
0-5	8	9	5	8	9	7	5	4	7
5-10	37	27	20	32	38	26	21	30	29
10-15	30	29	29	28	28	20	24	33	28
(cm s^{-1}) 15-20	13	19	24	14	7	11	16	14	15
20-25	5	11	14	6	6	13	11	6	9
25-30	1	0	4	0	3	9	9	1	3
SPRING									
Dir. frequency	11	7	7	8	11	13	21	18	
Mean speed	12.6	13.8	13.4	14.7	13.7	14.8	16.6	16.4	
0-5	12	12	14	12	13	11	5	6	11
5-10	32	29	32	26	29	30	22	22	28
10-15	29	25	23	32	33	30	30	27	29
(cm s^{-1}) 15-20	11	13	9	10	7	8	17	18	12
20-25	5	8	8	5	3	6	10	10	7
25-30	3	3	3	3	2	1	5	6	3
SUMMER									
Dir. frequency	7	5	7	8	11	17	25	15	
Mean speed	11.7	13.1	15.4	14.6	13.3	16.4	20.6	16.7	
0-5	18	14	11	13	13	9	5	9	11
5-10	25	23	23	18	22	17	12	18	20
10-15	27	24	19	24	26	23	19	24	23
(cm s^{-1}) 15-20	14	18	15	16	16	17	15	15	16
20-25	7	10	10	14	11	11	15	12	11
25-30	3	5	9	6	5	8	9	7	6
AUTUMN									
Dir. frequency	8	10	13	10	8	13	20	15	
Mean speed	17.6	16.8	17.4	17.9	19.6	24.9	27.9	24.7	
0-5	14	9	8	17	16	10	8	12	11
5-10	27	21	14	28	22	15	11	21	20
10-15	26	24	28	16	21	18	16	21	21
(cm s^{-1}) 15-20	10	15	17	10	14	14	15	11	13
20-25	5	14	15	8	7	9	10	5	9
25-30	1	6	7	3	1	4	6	2	4

INTERMEDIATE LAYER (30 m)

IKA j=44°17'-44°32' l=13°13'-13°38'	N	NE	E	SE	S	SW	W	NW	speed freq. (%)
WHOLE PERIOD									
Dir. frequency	9	5	7	14	14	14	18	20	
Mean speed	9.1	8.4	7.7	9.5	9.5	10.0	10.2	11.2	
0-5	30	36	35	25	26	26	23	18	27
5-10	30	32	37	32	31	29	30	28	31
10-15	23	15	18	27	25	23	26	27	23
(cm s^{-1}) 15-20	11	10	8	11	12	13	13	16	12
20-25	4	5	2	4	5	5	6	6	5
25-30	2	0	0	1	1	2	2	2	1
WINTER									
Dir. frequency	9	10	11	19	9	8	14	16	
Mean speed	8.9	11.0	9.1	9.6	8.0	8.5	8.0	9.2	
0-5	21	22	19	19	33	38	33	18	25
5-10	40	32	45	36	36	26	35	39	36
10-15	28	14	18	28	19	19	20	27	22
(cm s^{-1}) 15-20	3	17	13	13	6	9	8	11	10
20-25	4	12	2	2	3	4	2	1	4
25-30	0	0	0	0	0	0	0	0	0
SPRING									
Dir. frequency	8	4	4	12	15	13	18	23	
Mean speed	8.4	6.6	6.9	9.021	8.8	7.8	9.3	10.8	
0-5	31	40	42	38	22	28	19	14	27
5-10	31	36	35	30	38	42	37	32	36
10-15	24	21	17	7	28	23	31	31	26
(cm s^{-1}) 15-20	10	1	5	2	7	4	9	16	7
20-25	1	0	0	0	2	0	1	4	1
25-30	0	0	0		0	0	0	0	0
SUMMER									
Dir. frequency	9	4	6	14	14	12	16	21	
Mean speed	8.8	6.2	6.8	9.5	9.0	8.2	9.3	11.3	
0-5	35	50	44	27	28	34	28	23	34
5-10	26	32	31	28	30	31	30	22	29
10-15	22	14	18	26	25	22	25	26	22
(cm s^{-1}) 15-20	10	2	4	10	10	8	10	16	9
20-25	3	0	0	5	3	2	3	5	3
25-30	1	0	0	1	0	0	1	2	1
AUTUMN									
Dir. frequency	7	3	4	9	13	19	22	20	
Mean speed	10.1	7.7	7.5	9.7	11.3	12.8	12.4	12.6	
0-5	28	39	41	27	20	15	15	12	24
5-10	25	31	32	30	25	23	24	26	27
10-15	19	15	14	20	24	24	25	26	21
(cm s^{-1}) 15-20	16	8	7	12	17	19	18	18	14
20-25	6	2	3	6	8	9	10	9	7
25-30	2	0	1	2	2	4	0	3	2

BOTTOM LAYER (50 m)

IKA j=44°17'-44°32' l=13°13'-13°38'	N	NE	E	SE	S	SW	W	NW	speed freq. (%)
WHOLE PERIOD									
Dir. frequency	7	3	6	16	16	12	17	22	
Mean speed	5.8	4.1	6.0	8.1	7.5	7.3	7.5	8.5	
0-5	52	74	49	30	37	44	38	27	44
5-10	34	20	34	37	36	32	35	36	33
10-15	12	5	14	22	18	13	18	26	16
(cm s^{-1}) 15-20	2	1	2	8	6	7	6	9	5
20-25	1	0	1	2	2	2	2	2	1
25-30	0	0	0	0	1	1	1	0	0
WINTER									
Dir. frequency	7	2	3	10	20	17	21	17	
Mean speed	6.4	4.0	5.4	7.8	8.1	8.1	8.3	8.8	
0-5	40	71	49	17	26	31	28	25	37
5-10	42	28	40	43	44	42	40	35	39
10-15	12	0	8	22	20	12	20	27	15
(cm s^{-1}) 15-20	3	0	0	5	5	9	7	9	5
20-25	0	0	0	0	2	3	2	1	1
25-30	0	0	0	0	0	0	0	0	0
SPRING									
Dir. frequency	4	1	4	19	17	11	15	25	
Mean speed	6.9	5.7	6.0	9.0	6.6	5.5	7.1	9.1	
0-5	46	55	52	22	41	55	34	19	40
5-10	33	27	30	39	41	33	45	41	36
10-15	13	12	11	25	13	8	14	28	16
(cm s^{-1}) 15-20	3	3	3	10	2	2	3	8	4
20-25	1	0	1	2	0	0	1	1	0
25-30	0	0	0	0	0	0	0	0	0
SUMMER									
Dir. frequency	10	4	9	19	12	7	11	24	
Mean speed	5.4	4.2	6.1	7.7	5.9	5.4	7.0	7.7	
0-5	53	74	48	32	53	60	46	31	50
5-10	34	19	33	37	30	25	29	37	30
10-15	10	5	16	21	11	9	14	23	14
(cm s^{-1}) 15-20	0	0	2	7	3	3	4	6	3
20-25	0	0	0	1	0	0	2	1	0
25-30	0	0	0	0	0	0	1	0	0
AUTUMN									
Dir. frequency	6	2	7	14	15	13	18	21	
Mean speed	5.4	3.5	6.1	8.2	8.6	8.3	7.3	8.8	
0-5	59	81	49	34	32	40	40	29	46
5-10	25	14	32	32	30	26	30	30	27
10-15	11	3	14	19	20	17	20	26	16
(cm s^{-1}) 15-20	3	0	2	9	10	8	6	10	6
20-25	0	0	0	2	3	3	1	2	1
25-30	0	0	0	0	1	2	0	0	0